BOSE-EINSTEIN CONDENSATION AT LOWER DIMENSIONS

A THESIS SUBMITTED TO
THE GRADUATE SCHOOL OF NATURAL AND APPLIED SCIENCES
OF
THE MIDDLE EAST TECHNICAL UNIVERSITY

BY

SEVİLAY ÖZDEMİR

IN PARTIAL FULFILLMENT OF THE REQUIREMENTS FOR THE

DEGREE OF

MASTER OF SCIENCE

IN

THE DEPARTMENT OF PHYSICS

JANUARY 2004

Approval of the Graduate School of Natural and Applied Sciences.

Prof. Dr. Canan Özgen
Director

I certify that this thesis satisfies all the requirements as a thesis for the degree of Master of Science.

Prof. Dr. Sinan Bilikmen
Head of Department

This is to certify that we have read this thesis and that in our opinion it is fully adequate, in scope and quality, as a thesis for the degree of Master of Science.

Prof. Dr. Mehmet Tomak
Supervisor

Examining Committee Members

Prof. Dr. Sinan Bilikmen _____

Prof. Dr. Cevdet Tezcan _____

Prof. Dr. Mehmet Tomak _____

Assoc. Prof. Dr. Serhat Çakir _____

Assoc. Prof. Dr. Hatice Kökten _____

ABSTRACT

BOSE-EINSTEIN CONDENSATION AT LOWER DIMENSIONS

Özdemir, Sevilay

M.S., Department of Physics

Supervisor: Prof. Dr. Mehmet Tomak

January 2004, 53 pages

In this thesis, the properties of the Bose-Einstein condensation (BEC) in low dimensions are reviewed. Three dimensional weakly interacting Bose systems are examined by the variational method. The effects of both the attractive and the repulsive interatomic forces are studied. Thomas-Fermi approximation is applied to find the ground state energy and the chemical potential. The occurrence of the BEC in low dimensional systems, is studied for ideal gases confined by both harmonic and power-law potentials. The properties of BEC in highly anisotropic trap are investigated and the conditions for reduced dimensionality are derived.

Keywords: Gross-Pitaevskii formalism, reduced dimensionality, weakly interacting Bose gas, Thomas-Fermi approximation, variational method, nonlinear Schrödinger equation, highly anisotropic trap.

ÖZ

DÜŞÜK BOYUTLARDA BOSE-EINSTEIN YOĞUŞMASI

Özdemir, Sevilay
Yüksek Lisans, Fizik Bölümü
Tez Yöneticisi: Prof. Dr. Mehmet Tomak

Şubat 2004, 53 sayfa

Bu tezde, düşük boyutlardaki Bose-Einstein yoğuşmasının (BEY) özellikleri incelenmiştir. Zayıf etkileşimli üç boyutlu Bose sistemleri varyasyonel metodla incelenmiş ve atomlararası kuvvetlerin itici ve çekici olduğu durumlar analiz edilmiştir. Thomas-Fermi yaklaşımı uygulanarak taban enerjisi ve kimyasal potansiyel hesaplanmıştır. Düşük boyutlu sistemlerde, öncelikle harmonik ve üstel potansiyel altındaki ideal Bose gazlarında Bose-Einstein yoğuşmasının ortaya çıkması araştırılmış, yüksek-derecede anizotropik tuzaklardaki BEY çalışılmış ve indirgenmiş-boyutluluk için gereken koşullar ortaya konmuştur.

Anahtar Kelimeler: Gross-Pitaevskii formalizmi, indirgenmiş boyutluluk, zayıf etkileşimli Bose gazı, Thomas-Fermi yaklaşımı, varyasyon metodu, lineer olmayan Schrödinger denklemi, yüksek dereceli anizotropik tuzak.

To my lovely mother,

Şerif Özdemir

ACKNOWLEDGMENTS

I would like to express my sincere appreciation to Prof. Dr. Mehmet Tomak for his guidance and insight throughout the research.

I would like to thank to my sweetheart Hâldun Sevinçli for his encouragement and helpful discussions. I also thank my family and friends for their support.

TABLE OF CONTENTS

LIST OF FIGURES

CHAPTER I

INTRODUCTION

One of the long lasting problems in physics is the Bose-Einstein Condensation. It was predicted in 1925 [1] by Einstein, on the basis of the statistical description of the quanta of light by the Indian physicist S. N. Bose [2]. First experimental realization of Bose-Einstein Condensation (BEC) was achieved in 1995 in atomic gases [3], [4].

When a gas of bosonic atoms is cooled below a critical temperature T_c, a large fraction of the atoms condense to the state of lowest energy as a consequence of quantum statistical effects. In other words, when atoms are cooled to the point where the de Broglie wavelength, $\lambda_{dB} = (2\pi\hbar^2/mk_BT)^{1/2}$, is comparable to the interatomic separation, the atomic wavepackets overlap and the gas starts to become a "quantum soap" of indistinguishable particles. There is a quantum mechanical phase transition and it is called the Bose-Einstein Condensation (BEC).

After the discovery of superfluidity in liquid Helium [6],[7], F. London [8] considered that the superfluidity was a manifestation of BEC. Although there

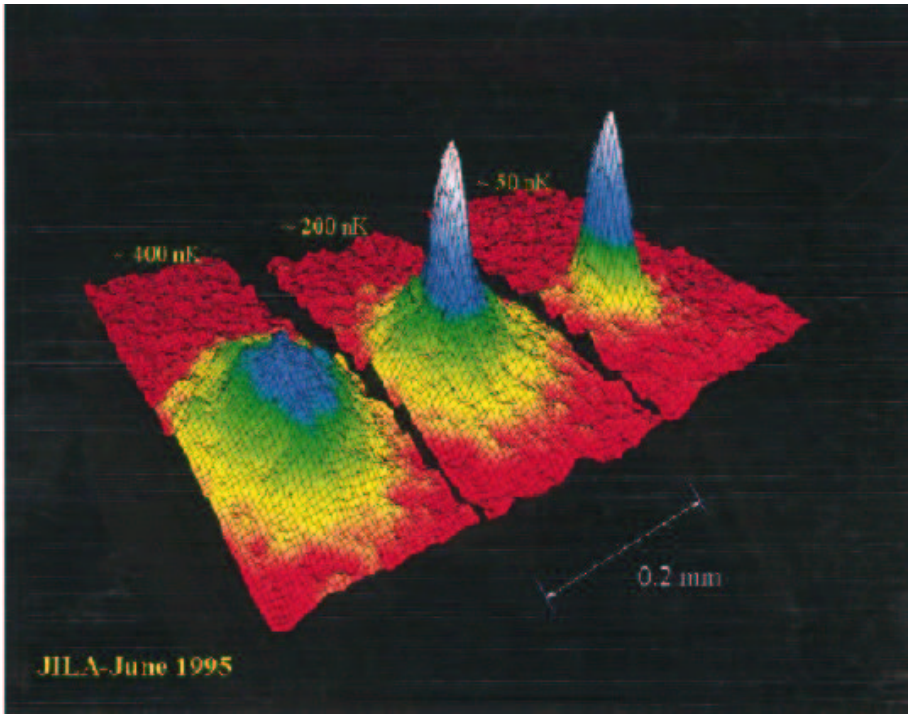

Figure I.1: Three density distributions of the expanded clouds of the rubidium atoms at three different temperatures. The appearance of the condensate is apparent as the narrow feature in the middle image. On the far right, nearly all the atoms in the sample are in the condensate. Colors represent the densities. From Cornell [11].

were several discussions for decades [9],[10] it is now recognized that the properties of superconductivity and superfluidity in both ^{3}He and ^{4}He are related to BEC [11].

The studies on the dilute atomic gases developed much later, starting from the 1970s, by the help of the new techniques in atomic physics and advanced cooling mechanisms.

In 1976 [12] spin-polarized Hydrogen was offered as a good candidate for realizing Bose-Einstein condensation since it has no bound states and would remain a gas down to zero temperature. This suggestion was followed by several

experiments [13],[14],[15]. In these experiments hydrogen atoms were first cooled in a dilution refrigerator, then trapped by a magnetic field and further cooled by evaporation. They were coming very close to BEC.

In the 1980s, laser cooling [16] and magneto-optical trapping [17] were developed to cool and trap atoms. Alkali atoms are well suited to laser-based methods since the available lasers can excite their optical transitions. Alkali atoms can be cooled to very low temperatures because of their favorable internal energy-level structure. After trapping, their temperature can be lowered further by evaporative cooling [18].

In these conditions, the equilibrium configuration of the system would be the solid phase. So that one has to preserve the system in a metastable gas phase for a sufficiently long time to observe BEC.

In the 1995, Cornell and Wieman at Boulder and Ketterle at MIT succeded in reaching temperatures and densities required to observe Bose-Einstein Condensation in vapors of ^{87}Rb [3] and ^{23}Na [4] by combining the laser and evaporative cooling for alkali atoms. They cooled the samples to a temperature of $\sim 2\mu K$. Recently, MIT group reported that they lowered to temperature to the order of $500pK$ [19]. In the same year, first signatures of the occurance of BEC in vapors of ^{7}Li were reported [20]. Bose-Einstein condensation was also achieved in other atomic species, spin-polarized Hydrogen [21], metastable ^{4}He [22],[23] and ^{41}K [24]. At least thirty groups have now created condensates [5].

One of the most important features of these trapped Bose gases is that they are inhomogeneous. This fact has several important consequences. First BEC shows up not only in momentum space but also in coordinate space. This property allows for the investigation of a series of quantities; like the temperature, energy and density, and so on.

After the realization of BEC in 1995, this field has grown explosively and

physicists from different areas of physics (atomic physics, quantum optics, condensed matter physics, etc.) are now working together.

The experimental observation of BEC has opened a new variety of important questions. At both experimental and theoretical level the possibility of interesting implications are demonstrated. Over the last years various studies on these systems are being performed such as collective excitations and rotational properties of the condensates, soliton behavior, quantized vortices and vortex lattices, interference and coherence phenomena, two component condensates, BEC in optical lattices as well as the reduced dimensional properties [18].

The aim of this thesis is to investigate the Bose-Einstein Condensation in lower dimensions. The study of the low dimensional systems is an important area in condensed matter physics because the spatial degree of freedom affects the properties of the phase transitions and collective oscillations. Hohenberg [26] has shown that BEC cannot occur in an "ideal" two dimensional system. Later it was shown that if the gas is confined by a spatially varying potential, BEC can occur. Recently, reduced dimensionality has been observed [25] in highly anisotropic traps. The experimental and theoretical interest is growing in this area.

In Chapter II, first the ideal Bose gas confined in a harmonic trap is studied and the results are compared to that of the ideal uniform gas. Important predictions can be made from this study such as the critical temperature. The formalism which is needed to describe the important features of these quantum gases is given. Next the theory is expressed in terms of a non-linear Schrödinger equation for the order parameter. The stationary and time dependent forms of this non-linear Schrödinger equation , the Gross-Pitaevskii Equation, are derived.

In Chapter III, three dimensional weakly interacting Bose gas confined in both spherically symmetric and cylindrically symmetric traps is examined by

the variational method. We study the effects of both the attractive and the repulsive interatomic forces. It is shown that the condensate will collapse if the interatomic forces are attractive. Finally Thomas-Fermi approximation is applied to the gas in cylindrically symmetric trap and the chemical potential and the radius of the cloud are calculated.

The next chapter includes the study of the low dimensional systems. First, we look for the occurrence of the Bose-Einstein Condensation in one and two dimensional ideal gasses confined by both harmonic and power-law potentials. The condensate fractions, critical temperatures and the energies per particle are calculated. Next we study the properties of the BEC in a highly anisotropic trap in effective 2D and 1D by the variational method. The total energy and the chemical potential are calculated in cigar and pancake geometries. Finally, the conditions for reduced dimensionality are derived and we compare the release energy with the experimentally observed value. In Chapter V, a concluding discussion is given.

CHAPTER II

BASIC FORMALISM

In this chapter, the formalism which is required for the study of the BEC in various dimensions is summarized. The ideal Bose gas confined by harmonic potential is studied. We find the condensate fraction, total energy and the specific heat for ideal uniform case. Then weakly interacting gases are examined. Time-dependent and stationary Gross-Pitaevskii equations are derived. The energy functional is obtained, the ground state properties and the interaction effects are discussed.

II.1 The Ideal Bose Gas

II.1.1 The Ideal Bose Gas In A Harmonic Trap

The confining potential for the ideal Bose gas in a harmonic trap can be written in the quadratic form as

$$V_{ext}(\mathbf{r}) = \frac{m}{2}(\omega_x^2 x^2 + \omega_y^2 y^2 + \omega_z^2 z^2), \tag{II.1}$$

where ω_x, ω_y and ω_z are the oscillator frequencies. If we neglect the atom-atom interactions then almost all predictions are analytical and relatively simple.

The many-body Hamiltonian is the sum of single-particle Hamiltonians whose eigenvalues have the form,

$$\epsilon_{n_x n_y n_z} = \left(n_x + \frac{1}{2}\right)\hbar\omega_x + \left(n_y + \frac{1}{2}\right)\hbar\omega_y + \left(n_z + \frac{1}{2}\right)\hbar\omega_z, \tag{II.2}$$

where n_x, n_y, n_z are nonnegative integers. By putting all the particles in the lowest single particle state ($n_x = n_y = n_z = 0$) we get the ground state wave function as $\varphi(\mathbf{r}_1, ..., \mathbf{r}_N) = \prod_i \varphi_0(\mathbf{r}_i)$, where $\varphi_0(\mathbf{r}_i)$ is given by

$$\varphi_0(\mathbf{r}) = \left(\frac{m\omega_{ho}}{\pi\hbar}\right)^{3/4} \exp\left[-\frac{m}{2\hbar}(\omega_x x^2 + \omega_y y^2 + \omega_z z^2)\right], \tag{II.3}$$

where the geometric average of the oscillator frequencies is $\omega_{ho} = (\omega_x\omega_y\omega_z)^{1/3}$. The density distribution becomes $\rho(\mathbf{r}) = N|\varphi_0(\mathbf{r})|^2$. The size of the cloud is fixed by the harmonic oscillator length,

$$a_{ho} = \left(\frac{\hbar}{m\omega_{ho}}\right)^{1/2}. \tag{II.4}$$

This is the first important length scale of the system. In the available experiment, it is typically of the order of $1\mu m$ [27]. At finite temperatures only a fraction of the atoms occupy the lowest state. The others are thermally distributed in the excited states at higher energies. The radius of the thermal cloud is larger than a_{ho}.

Bose-Einstein Condensation in harmonic traps shows up with the appearance of a sharp peak in the central region of the density distribution.

At temperature T, the total number of particles is given, in the grand canonical ensemble, by

$$N = \sum_{n_x, n_y, n_z} \frac{1}{\exp[\beta(\epsilon_{n_x n_y n_z} - \mu)] - 1}, \tag{II.5}$$

while the total energy is

$$E = \sum_{n_x, n_y, n_z} \frac{\epsilon_{n_x n_y n_z}}{\exp[\beta(\epsilon_{n_x n_y n_z} - \mu)] - 1}, \tag{II.6}$$

where μ is the chemical potential and $\beta = (kT)^{-1}$. Below a given temperature the population of the lowest state becomes macroscopic. This corresponds to the realization of BEC.

Because of the fact that these systems have finite sizes and they are inhomogeneous, there are several problems. For instance, we cannot use the common definition of the thermodynamic limit (increasing N and volume with the average density kept constant) for trapped gases.

We separate out the the lowest eigenvalue ϵ_{000} from the sum (II.5) and call N_0 the number of particles in this state. This number can be macroscopic when the chemical potential becomes equal to the lowest energy, $\mu \to \mu_c = 3\hbar\overline{\omega}/2$ where arithmetic average of the oscillator frequencies is $\overline{\omega} = (\omega_x + \omega_y + \omega_z)/3$. Substituting this into the sum, we can write

$$N - N_0 = \sum_{n_x,n_y,n_z \neq 0} \frac{1}{\exp[\beta(\omega_x n_x + \omega_y n_y + \omega_z n_z)] - 1}. \tag{II.7}$$

When $N \to \infty$,

$$N - N_0 = \int_0^\infty \frac{dn_x\, dn_y\, dn_z}{\exp[\beta(\omega_x n_x + \omega_y n_y + \omega_z n_z)] - 1}. \tag{II.8}$$

This assumption corresponds to a semiclassical description of the excited states. For its validity, the excitation energies must be much larger than the level spacing fixed by oscillator frequencies. If the number of trapped atoms is large and $kT \ll \hbar\omega_{ho}$ this semiclassical approximation is accurate.

By changing variables ($\beta\hbar\omega_x n_x = \tilde{n_x}$, etc.) and using the definition of Riemann Zeta function(Appendix A), we get

$$N - N_0 = \left(\frac{kT}{\hbar\omega_{ho}}\right)^3 \zeta(3), \tag{II.9}$$

where $\zeta(n)$ is the Riemann Zeta function.

By imposing that $N_0 \to 0$ at the transition we can find the temperature as

$$kT_c = \hbar\omega_{ho}\left(\frac{N}{\zeta(3)}\right)^{1/3} = 0.94\,\hbar\omega_{ho}N^{1/3}. \tag{II.10}$$

For the temperatures above T_c the chemical potential is less than μ_c and becomes N dependent and the population of the lowest state is of the order of 1. By letting $N \to \infty$ and $\omega_{ho} \to 0$ while keeping the product $N\omega_{ho}^3$ constant we can obtain the proper thermodynamic limit for these systems. The transition temperature (II.10) is well defined in this thermodynamic limit. Inserting this expression into equation (II.9) we get the condensate fraction for $T < T_c$,

$$\frac{N_0}{N} = 1 - \left(\frac{T}{T_c}\right)^3. \tag{II.11}$$

Substituting the density of states $\rho(\epsilon) = (1/2)(\hbar\omega_{ho})^{-3}\epsilon^2$ into the integral $E = \int_0^\infty d\epsilon\, \rho(\epsilon)\epsilon/[\exp(\beta\epsilon) - 1]$ we can find the energy as

$$E = 3\zeta(4)\frac{(kT)^4}{(\hbar\omega_{ho})^3}, \tag{II.12}$$

and substitution of the transition temperature gives

$$\frac{E}{NkT_c} = \frac{3\zeta(4)}{\zeta(3)}\left(\frac{T}{T_c}\right)^4. \tag{II.13}$$

Starting from this energy we can calculate the specific heat

$$C_v = \frac{dE}{dT} = Nk\frac{12\zeta(4)}{\zeta(3)}\left(\frac{T}{T_c}\right)^3. \tag{II.14}$$

These results can be compared with that of uniform Bose gases. In this case, the eigenstates of the Hamiltonian are plane waves with energy $\epsilon = p^2/2m$. The sum (II.5) yields $N_0/N = 1 - (T/T_c)^{3/2}$ and the energy is $E/(Nk_BT_c) = 0.77(T/T_c)^{5/2}$ while the specific heat is given by $C_V = 1.93Nk_B(T/T_c)^{3/2}$. In the Figures (II.1, II.2, II.3) one can see the comparison of the condensate fractions, energies and the specific heats of uniform and harmonically confined gases.

Density of the thermal particles $\rho_T(\mathbf{r})$ and the condensate density, $\rho_0(\mathbf{r}) = N_0|\varphi_0(\mathbf{r})|^2$, gives the total density $\rho(\mathbf{r}) = \rho_0(\mathbf{r}) + \rho_T(\mathbf{r})$. In the thermodynamic limit and when $T < T_c$ the thermal density is given by

$$\rho_T(\mathbf{r}) = \int d\mathbf{p}(2\pi\hbar)^{-3}[\exp(\beta\epsilon(\mathbf{p},\mathbf{r})) - 1]^{-1}, \tag{II.15}$$

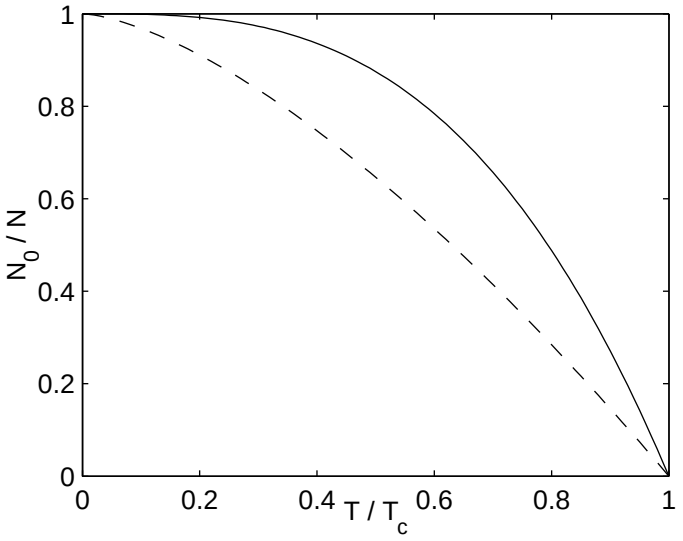

Figure II.1: Condensate fraction as a function of T/T_c. Dashed line stands for the Ideal uniform Bose Gas and solid line for Bose gas in a Harmonic trap.

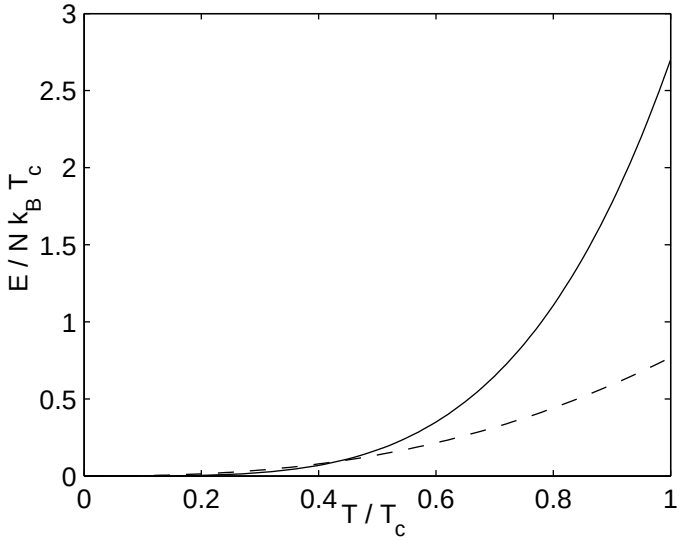

Figure II.2: Energy per particle as a function of T/T_c. Dashed line shows the ideal case, solid line stands for harmonic trapping.

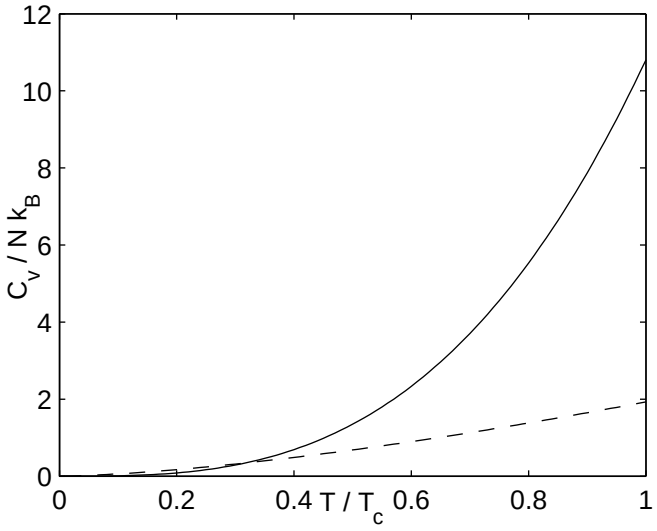

Figure II.3: Heat capacity as a function of T/T_c. Dashed line:Ideal case. Solid line: Harmonic potential case.

where $\epsilon(\mathbf{p},\mathbf{r}) = (p^2/2m) + V_{ext}(\mathbf{r})$ is the semiclassical energy in phase space. By changing variables ($\beta p^2/2m = x$) we get

$$\rho_T(\mathbf{r}) = \lambda_T^{-3} g_{3/2}(\mathrm{e}^{-\beta \mathrm{V_{ext}(\mathbf{r})}}), \tag{II.16}$$

where $\lambda_T = (2\pi\hbar^2/mkT)^{1/2}$ is the thermal wavelength and the function $g_{3/2}(\mathbf{r})$ belongs to Bose functions (Appendix A). By integrating $\rho_T(\mathbf{r})$ over space one gets again the number of thermally depleted atoms $N - N_0 = N(T/T_c)^3$, consistent with Equation (II.11). In a similar way the distribution of thermal particles in momentum space can be obtained as

$$\rho_T(\mathbf{p}) = (\lambda_{\mathbf{T}}\mathbf{m}\omega_{\mathbf{ho}})^{-\mathbf{3}}\mathbf{g_{3/2}}(\mathrm{e}^{-\beta \mathrm{p^2/2m}}). \tag{II.17}$$

The above analysis shows that the existence of two relevant scales of energy for the ideal gas. the transition temperature kT_c and the average level spacing $\hbar\omega_{ho}$. It is clearly seen that kT_c can be much larger than $\hbar\omega_{ho}$ from expression (II.10). In the available traps, with N ranging from a few thousands to several millions,

the transition temperature is 20 to 200 times larger than $\hbar\omega_{ho}$. This also means that the semiclassical approximation is expected to work well in these systems on a wide and useful range of temperatures. It is also seen that the chemical potential is of the order of $\hbar\omega_{ho}$ for the ideal gas. However, its value depends on the atom-atom interaction and provide a third important scale of energy.

The noninteracting harmonic oscillator model has guided experimentalists to the proper value of the critical temperature. Actually the measured transition temperature was found to be very close to this value (II.10) and below the critical temperature the occupation of the condensate becomes macroscopically large as calculated above [28].

II.2 Effects Of Interaction

Gross-Pitaevskii Equation

The many-body Hamiltonian describing the system consisting of N interacting bosons with trapping potential V_{ext} is given, in second quantization, by [27]

$$\begin{aligned} \hat{H} &= \int d\mathbf{r}\, \hat{\Psi}^\dagger(\mathbf{r}) \left[-\frac{\hbar^2}{2m}\nabla^2 + V_{ext}(\mathbf{r}) \right] \hat{\Psi} \\ &+ \frac{1}{2}\int d\mathbf{r}\, d\mathbf{r}' \hat{\Psi}^\dagger(\mathbf{r})\hat{\Psi}^\dagger(\mathbf{r}')V(\mathbf{r}-\mathbf{r}')\hat{\Psi}(\mathbf{r}')\hat{\Psi}(\mathbf{r}), \end{aligned} \tag{II.18}$$

where $\hat{\Psi}(\mathbf{r})$ and $\hat{\Psi}^\dagger(\mathbf{r})$ are the boson field operators that annihilate and create a particle at the position $\mathbf{r}$ respectively and $V(\mathbf{r}-\mathbf{r}')$ is the two-body interatomic potential. The thermodynamic properties of the system and its ground state can be directly calculated from this Hamiltonian (II.18).

There are a number of approaches to work with the many-body Hamiltonian. Schneider and Feder [29] has used numerical calculations based on a discrete variable representation of the Hamiltonian. Other approaches like mean-field theories are developed for interacting systems in order to overcome the problem of solving the full many-body Schrödinger equation exactly. Making use of the

mean-field theories, one can avoid the heavy numerical work and the system can be understood in terms of parameters having clear physical meanings.

The basic idea of a mean-field description for a dilute Bose gas was formulated by Bogoluibov[30]. Separation of the condensate contribution from the bosonic field operator is the key point of this formalism. In general, the field operator can be written as $\hat{\Psi}(\mathbf{r}) = \sum_\alpha \Psi_\alpha(\mathbf{r}) a_\alpha$, where $\Psi_\alpha(\mathbf{r})$ are single-particle wave functions and a_α are the corresponding annihilation operators. The bosonic creation and annihilation operators $a_\alpha^\dagger$ and a_α are defined as

$$a_\alpha^\dagger |n_0, n_1, ..., n_\alpha, ...\rangle = \sqrt{n_\alpha + 1}\,|n_0, n_1, ..., n_\alpha + 1, ...\rangle, \tag{II.19}$$

$$a_\alpha |n_0, n_1, ..., n_\alpha, ...\rangle = \sqrt{n_\alpha}\,|n_0, n_1, ..., n_\alpha - 1, ...\rangle, \tag{II.20}$$

where n_α are the eigenvalues of the operator $\hat{n}_\alpha = a_\alpha^\dagger a_\alpha$ giving the number of atoms in the single-particle $\alpha-$state. These operators obey the general commutation rules:

$$[a_\alpha, a_\beta^\dagger] = \delta_{\alpha\beta}, \quad [a_\alpha, a_\beta] = 0, \quad [a_\alpha^\dagger, a_\beta^\dagger] = 0. \tag{II.21}$$

Bose-Einstein condensation occurs when the number of atoms n_0 of a particular single-particle state becomes very large: $n_0 \equiv N_0 \gg 1$ and the ratio N_0/N remains finite in the thermodynamic limit $N \to \infty$. In this limit states with N_0 and $N_0 \pm 1 \approx N_0$ correspond to the same physical configuration. Consequently the operators $a_0^\dagger$ and a_0 can be treated like numbers: $a_0 = a_0^\dagger = \sqrt{N_0}$.

Bose-Einstein condensation occurs in the single-particle state $\Psi_0 = 1/\sqrt{V}$ having zero momentum for a uniform gas in volume V. Then, $\Psi(\mathbf{r})$ can be decomposed in the form

$$\Psi(\mathbf{r}) = \sqrt{N_0/V} + \Psi'(\mathbf{r}). \tag{II.22}$$

In the case of nonuniform and time-dependent configuration the generalization of the Bogoliubov formalism is given by

$$\hat{\Psi}(\mathbf{r}, t) = \Phi(\mathbf{r}, t) + \Psi'(\mathbf{r}, t), \tag{II.23}$$

here $\Phi(\mathbf{r},t)$ is a complex function and defined as the expectation value of the field operator: $\Phi(\mathbf{r},t) \equiv \langle \hat{\Psi}(\mathbf{r},t) \rangle$. Its modulus fixes the condensate density

$$\rho_0(\mathbf{r},t) = |\Phi(\mathbf{r},t)|^2. \tag{II.24}$$

The function $\Phi(\mathbf{r},t)$ is a classical field having the meaning of order parameter. It is often called the "wave function of the condensate".

If Ψ' is small, that is the depletion of the condensate is small, the decomposition of field operator (II.23)becomes useful. The time evolution of the field operator $\hat{\Psi}(\mathbf{r},t)$ is written by using Heisenberg equations with the many-body Hamiltonian (II.18) to derive the equation for $\Phi(\mathbf{r},t)$;

$$\begin{aligned} i\hbar\frac{\partial}{\partial t}\hat{\Psi}(\mathbf{r},t) &= [\hat{\Psi},\hat{H}], \qquad \text{(II.25)} \\ &= \left[-\frac{\hbar^2\nabla^2}{2m} + V_{ext} + \int d\mathbf{r}'\hat{\Psi}^\dagger(\mathbf{r}',t)V(\mathbf{r}'-\mathbf{r})\hat{\Psi}(\mathbf{r}',t)\right]\hat{\Psi}(\mathbf{r},t). \end{aligned}$$

Then the operator $\hat{\Psi}$ is replaced with the classical field Φ.For the interaction term in the integral this replacement is a poor approximation for the short distances. However, in the case of dilute and cold gas only binary collisions at low energy is relevant and these collisions characterized by a single parameter, the s-wave scattering length. Then a proper expression can be obtained for the interaction term independent of the two-body potential. Then $V(\mathbf{r}'-\mathbf{r})$ can be replaced with an effective interaction

$$V(\mathbf{r}'-\mathbf{r}) = g\delta(\mathbf{r}'-\mathbf{r}), \tag{II.26}$$

where the coupling constant g is related to the scattering length a through

$$g = \frac{4\pi\hbar^2 a}{m}. \tag{II.27}$$

Using the effective potential (II.26) in equation (II.25) order parameter can be written as

$$i\hbar\frac{\partial}{\partial t}\Phi(\mathbf{r},t) = \left[-\frac{\hbar^2}{2m} + V_{ext}(\mathbf{r}) + g|\Phi(\mathbf{r},t)|^2\right]\Phi(\mathbf{r},t). \tag{II.28}$$

This equation is known as Gross-Pitaevskii (GP) equation, was derived independently by Gross [31, 32] and Pitaevskii [33].

Validity of the GP equation is based on the condition that s-wave scattering length be much smaller than the average distance between atoms and that the number of atoms in the condensate be much larger than 1.

The GP equation is also obtained by a variational procedure

$$i\hbar\frac{\partial}{\partial t}\Phi = \frac{\delta E}{\delta \Phi^*}, \tag{II.29}$$

where the energy functional is given by

$$E[\Phi] = \int d\mathbf{r}\left[\frac{\hbar^2}{2m}|\nabla\Phi|^2 + V_{ext}(\mathbf{r})|\Phi|^2 + \frac{g}{2}|\Phi|^4\right]. \tag{II.30}$$

The first term in the integral is the kinetic energy of the condensate E_{kin}, the second is the harmonic oscillator energy E_{ho} and the last one is the mean-field interaction energy E_{int}. The validity of the dilute gas approximation is controlled by the dimensionless parameter. The number of particles in a "scattering volume" $|a|^3$. This can be written as $\overline{\rho}|a|^3$, where $\overline{\rho}$ is the average density of the gas. When $\overline{\rho}|a|^3 \ll 1$ the system is dilute or weakly interacting.

However the smallness of the parameter $\overline{\rho}|a|^3$ does not always mean that the interaction effects are small. These effects have to be compared with the kinetic energy of the atoms in the trap. One can show the importance of the atom-atom interaction on the ground state of the harmonic oscillator by calculating the interaction energy, E_{int}. This energy can be written as, $gN\overline{\rho}$, and the average density is of the order of N/a_{ho}^3 where $a_{ho} = (\hbar/m\omega_{ho})^{1/2}$ is harmonic oscillator length. Thus $E_{int} \propto N^2|a|/a_{ho}^3$. Kinetic energy is of the order of $N\hbar\omega_{ho}$, thus $E_{kin} \propto Na_{ho}^{-2}$. Comparing these two energies one can find that

$$\frac{E_{int}}{E_{kin}} \propto \frac{N|a|}{a_{ho}}. \tag{II.31}$$

This parameter can easily be larger than 1 even if $\overline{\rho}|a|^3 \ll 1$, so that very dilute gases can also exhibit an important non-ideal behavior.

Because of the assumption $\hat{\Psi}' = 0$, the above formalism is strictly valid only in the limit of zero temperature, that is all the particles are in the condensate.

II.3 The Ground State Solution

The scattering length in the Gross-Pitaevskii equation can be positive or negative and its sign and magnitude depends on the atom-atom potential. Positive and negative values of a correspond to an effective repulsion and attraction between the atoms, respectively. When $N|a|/a_{ho} \gg 1$, in other words when the interaction energy is much greater than the kinetic energy, the change can be dramatic. The central density of the condensate is raised (lowered) by an attractive (repulsive) interaction and as a result the radius of the cloud decreases (increases). This effect of the interaction has important consequences not only for the structure of the ground state but also for the thermodynamic properties of the system.

By using the formalism of the mean-field theory the ground state can be obtained. One can write the condensate wave function as $\Phi(\mathbf{r}, t) = \varphi(\mathbf{r})\mathrm{e}^{-\mathrm{i}\mu t/\hbar}$, where μ is the chemical potential. φ is real and normalized to the total number of particles, $\int d\mathbf{r}\varphi^2(\mathbf{r}) = N_0 = N$. Then the Gross-Pitaevskii equation (II.28) becomes

$$\left(-\frac{\hbar^2\nabla^2}{2m} + V_{ext}(\mathbf{r}) + g\varphi^2(\mathbf{r})\right)\varphi(\mathbf{r}) = \mu\varphi(\mathbf{r}). \tag{II.32}$$

Nonlinearity is coming from the mean-field term proportional to the particle density $\rho(\mathbf{r}) = \varphi^2(\mathbf{r})$ and this equation has the form of a "nonlinear Schrödinger equation". When $g = 0$, i.e. when there is no interaction, this equation reduces to the usual Schrödinger equation.

For nonlinear partial differential equations, several approximation procedures exist[34]. We used the variational method based on reducing the infinite-dimensional problem of the partial differential equation to a second order ordinary differential equation for the variational parameter that characterizes the solution. This is done by taking an appropriate variational wave function with a fixed shape but some free parameters. The validity of the variational results is only qualitative, i.e. if the shape of the actual solution is close to the variational wave function, the results obtained with variational method will be in agreement with the real solution. One should also interested in the existence and and the uniqueness of the minimum point. Here qualitative properties include continuous dependence of the minimum point. Another important property consists of the convergence of any minimizing sequence to a minimum point. For minimization problems the functional to be minimized is larger than certain quantities, which are necessarily bounded for any minimizing sequence. There are two fundamental techniques to prove the existence of a solution. The energy functional (II.30) is convex then we used the direct method.

The solution of the equation (II.32) minimizes the energy functional (II.30) for a fixed number of particles. Since the ground state has no currents, energy is a function of density only and can be written as

$$\begin{aligned} E[\rho] &= \int d\mathbf{r} \left[\frac{\hbar^2}{2m} |\nabla \sqrt{\rho}|^2 + \rho V_{ext}(\mathbf{r}) + \frac{g\rho^2}{2} \right], \\ &= E_{kin} + E_{ho} + E_{int}. \end{aligned} \tag{II.33}$$

The first term in the integral represents the quantum kinetic energy and it is usually called as "quantum pressure". For uniform systems it vanishes.

We can find the expression for the chemical potential by direct integration of the stationary GP equation (II.32)

$$\mu = \frac{E_{kin} + E_{ho} + 2E_{int}}{N}. \tag{II.34}$$

The balance between the quantum pressure and interaction energy of the condensate fixes the healing length. This is the minimum distance over which the order parameter can heal. It is also in a sense the length over which the gas heals from internal collisions. If the density of the condensate grows from 0 to ρ in a distance ξ, the quantum pressure in (II.33) with $p = \hbar/\xi$ is of the order of $\hbar^2/(2m\xi^2)$ and the interaction energy in (II.33) ($E_{int} = g\rho$) is of the order of $4\pi\hbar^2 a\rho/m$. By equating them one gets

$$\xi = (8\pi\rho a)^{-1/2}. \tag{II.35}$$

This is the well known result for weakly interacting Bose gas. One can see that under normal BEC conditions ($\overline{\rho}|a|^3 \ll 1$) ξ is large compared to $|a|$ (but generally small compared to typical trap dimensions).

CHAPTER III

THREE DIMENSIONAL WEAKLY INTERACTING BOSE GAS

In this chapter, the three dimensional Bose gas which has an attractive interaction ($a < 0$) is studied in a spherically symmetric harmonic trap. Using the variational method, energy per particle is calculated and it is shown that the condensate will collapse if the interatomic forces are attractive. Second, the gas with repulsive interatomic forces ($a > 0$) is examined in a cylindrically symmetric trap using the same method.Energy per particle is calculated and plotted for various values of the interaction parameter and Thomas-Fermi approximation is applied to find the chemical potential and the radius of the cloud.

III.1 Spherically Symmetric Trap

One can determine the behavior of the gas which has a negative scattering length ($a < 0$) in a spherical trap by means of the equation (II.30) in Chapter II . This can be done by means of Gaussian trial functions. We take a variational trial

wave function as [27]

$$\varphi(r) = \left(\frac{N}{w^3 a_{ho}^3 \pi^{3/2}}\right)^{1/2} \exp\left(-\frac{r^2}{2w^2 a_{ho}^2}\right), \tag{III.1}$$

where w is a dimensionless variational parameter which fixes the width of the condensate. Substituting this wave function into the energy functional (II.30)

$$\begin{aligned} E[\varphi] &= \int d\mathbf{r} \left[\frac{\hbar^2}{2m}\left(\frac{N}{w^7 a_{ho}^7 \pi^{3/2}} r^2 \mathrm{e}^{-\mathrm{r}^2/\mathrm{w}^2\mathrm{a}_{\mathrm{ho}}^2}\right) + \frac{m}{2}\omega_{ho}^2 r^2 \left(\frac{N}{w^3 a_{ho}^3 \pi^{3/2}} \mathrm{e}^{-\mathrm{r}^2/\mathrm{w}^2\mathrm{a}_{\mathrm{ho}}^2}\right)\right. \\ &+ \left.\frac{2\pi\hbar^2|a|}{m}\frac{N^2}{w^6 a_{ho}^6 \pi^3} \mathrm{e}^{-2\mathrm{r}^2/\mathrm{w}^2\mathrm{a}_{\mathrm{ho}}^2}\right]. \end{aligned} \tag{III.2}$$

The above integral can be treated as the sum of three integrals; $I = I_1 + I_2 + I_3$. In the first one, we take the polar and azimuthal integrals and we make the change of variables $x = r^2$ which gives us

$$I_1 = \frac{N\hbar^2}{m w^7 a_{ho}^7 \pi^{1/2}} \int_0^\infty x^{3/2} \mathrm{e}^{-\alpha \mathrm{x}} \mathrm{dx}, \tag{III.3}$$

where $\alpha = 1/w^2 a_{ho}^2$. Then recalling the definition of the Gamma function(A) $\int_0^\infty r^n \mathrm{e}^{-\gamma \mathrm{r}} \mathrm{dr} = \Gamma(\mathrm{n}+1)/\gamma^{\mathrm{n}+1}$, we get

$$I_1 = \frac{3}{4}\frac{N\hbar^2}{m w^2 a_{ho}^2}. \tag{III.4}$$

Applying the same procedure to I_2 and I_3, the energy is obtained as

$$E = \frac{3N\hbar^2}{4m w^2 a_{ho}^2} + \frac{3Nm\omega_{ho}^2 w^2 a_{ho}^2}{4} + \frac{N^2\hbar^2|a|}{(2\pi)^{1/2} m w^3 a_{ho}^3}. \tag{III.5}$$

Thus the energy per particle in terms of $\hbar\omega_{ho}$ is

$$\frac{E}{N\hbar\omega_{ho}} = \frac{3}{4}(w^{-2} + w^2) - (2\pi)^{-1/2}\frac{N|a|}{a_{ho}} w^{-3}. \tag{III.6}$$

This energy is plotted in Figure (III.1) as a function of w for several values of the parameter $N|a|/a_{ho}$.

If the forces are attractive ($a < 0$), the gas tends to increase its density in the center of the trap to lower the interaction energy. The kinetic energy resists

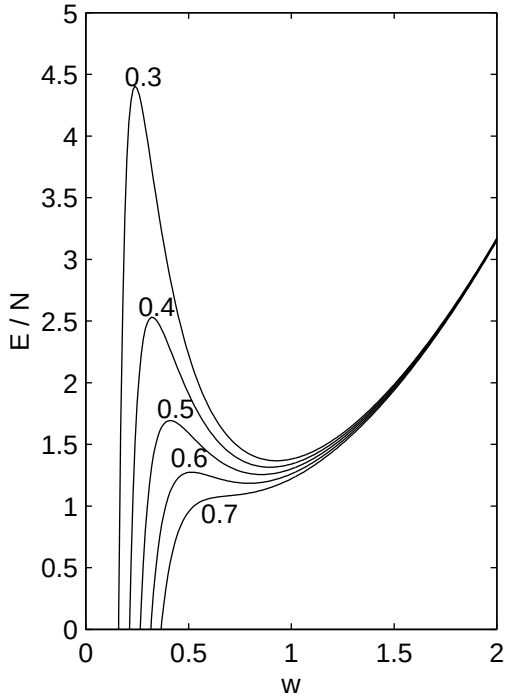

Figure III.1: Energy per particle, in units of $\hbar\omega_{ho}$, for atoms in a spherical trap interacting with attractive forces as a function of the effective width w. Curves are plotted for several values of the parameter $N|a|/a_{ho}$.

this to stabilize the system. If the central density grows too much, the kinetic energy can not avoid the collapse of the gas. The collapse is expected to occur when the number of particles in the condensate exceeds a critical value N_{cr} of the order of $a_{ho}/|a|$. To find N_{cr} we analyze the first and the second derivatives of the energy (III.6)and equate them to zero. Finally, we get $w_{cr} \approx 0.669$ and $N_{cr}|a|/a_{ho} \approx 0.671$.

From the Figure III.1, one can see that when $N_{cr}|a|/a_{ho}$ exceeds a critical value, the local minimum disappears. Ruprecht et al. [35] found $N_{cr}|a|/a_{ho} = 0.575$ for a spherical trap by means of the GP equation. Above N_{cr} the minimum no longer exists and the GP equation has no solution.

III.2 Cylindrically Symmetric Trap

Consider the gas which is trapped in an effective harmonic well cylindrically symmetric about the z-axis and has repulsive interatomic forces. The oscillators are characterized by lengths $a_\perp = (\hbar/m\omega_\perp^0)^{1/2}$ and $a_z = (\hbar/m\omega_z^0)^{1/2}$, where m is the atomic mass, $\omega_\perp^0$ and ω_z^0 are the angular frequencies in the transverse xy-plane and axial (z)direction,respectively. In the absence of interparticle interactions the lowest single-particle state has the wave function [36]

$$\phi_0(\mathbf{r}) = \frac{1}{\pi^{3/4} a_\perp a_z^{1/2}} \mathrm{e}^{-\mathrm{m}(\omega_\perp^0 \mathrm{r}_\perp^2 + \omega_z^0 \mathrm{z}^2)/2\hbar}, \tag{III.7}$$

where $r_\perp$ is the component of $\mathbf{r}$ in the xy-plane. The density distribution at zero temperature $\rho_0(\mathbf{r}) = N\phi_0(\mathbf{r})$ is Gaussian. However, interatomic interactions modify the particle structure in the well.

The density is reduced because of the repulsive interactions. The cloud of particles expands in the transverse direction as the number of particles increases. Because there are weak restoring forces with further increase in the number, the cloud expands in z-direction. The balance between the harmonic oscillator and the interaction energies determines the size of the cloud. Neglecting the anisotropy of the oscillator potential one can see the physics of this balance. Assuming the cloud occupies a region of radius $\approx R$, then $\rho \approx N/R^3$, we found the scale of harmonic oscillator energy per particle $\approx (4\pi\hbar^2 a/m)N/R^3$. If we equate them, the characteristic length scale is $\approx a_\perp \varsigma$, where the dimensionless parameter characterizing the system is

$$\varsigma \equiv (8\pi N a/a_\perp)^{1/5} \tag{III.8}$$

under the conditions of the trap with large N, $\varsigma \gg 1$.

To see the interaction effects we examine the ground state of the system in terms of its order parameter $\varphi(\mathbf{r})$. For a solution we take φ in the form of the

ground state wave function (III.7)

$$\varphi(\mathbf{r}) = N^{1/2}\omega_{\perp}^{1/2}\omega_z^{1/4}\left(\frac{m}{\pi\hbar}\right)^{3/4} \mathrm{e}^{-\mathrm{m}(\omega_{\perp}\mathrm{r}_{\perp}^2+\omega_{\mathrm{z}}\mathrm{z}^2)/2\hbar} \tag{III.9}$$

with effective frequencies $\omega_{\perp}$ and ω_z that are treated as variational parameters. Substitution of this φ into energy functional (II.30)and use of $g = 4\pi\hbar^2 a/m$ yields

$$\begin{aligned} E(\varphi) = \int \quad d^3r \quad & \left[\frac{N\omega_{\perp}\omega_z^{1/2}m}{2}\left(\frac{m}{\pi\hbar}\right)^{3/2}(\omega_{\perp}^2 r_{\perp}^2 + \omega_z^2 z^2)\mathrm{e}^{-\mathrm{m}(\omega_{\perp}\mathrm{r}_{\perp}^2+\omega_{\mathrm{z}}\mathrm{z}^2)/\hbar}\right. \\ + \quad & \frac{N\omega_{\perp}\omega_z^{1/2}m}{2}\left(\frac{m}{\pi\hbar}\right)^{3/2}[(\omega_{\perp}^0)^2 r_{\perp}^2 + (\omega_z^0)^2 z^2]\mathrm{e}^{-\mathrm{m}(\omega_{\perp}\mathrm{r}_{\perp}^2+\omega_{\mathrm{z}}\mathrm{z}^2)/\hbar} \\ + \quad & \left.\frac{2\pi\hbar^2 a N^2\omega_{\perp}^2\omega_z}{m}\left(\frac{m}{\pi\hbar}\right)^{3}\mathrm{e}^{-2\mathrm{m}(\omega_{\perp}\mathrm{r}_{\perp}^2+\omega_{\mathrm{z}}\mathrm{z}^2)/\hbar}\right]. \end{aligned} \tag{III.10}$$

By using the similar methods which are used in the previous section we can solve this integral. We treated this integral as a sum of five different integrals. By making use of the definition of the Gamma function and making change of variables one can find the ground state energy as

$$E(\omega_{\perp},\omega_z) = N\hbar\left(\frac{\omega_{\perp}}{2} + \frac{\omega_z}{4} + \frac{(\omega_{\perp}^0)^2}{2\omega_{\perp}} + \frac{(\omega_z^0)^2}{4\omega_z} + \frac{Nam^{1/2}}{(2\pi\hbar)^{1/2}}\omega_{\perp}\omega_z^{1/2}\right). \tag{III.11}$$

Minimizing the energy with respect to $\omega_{\perp}$ one gets,

$$N\hbar\left(\frac{1}{2} - \frac{(\omega_{\perp}^0)^2}{2\omega_{\perp}^2} + \frac{Nam^{1/2}}{(2\pi\hbar)^{1/2}}\omega_z^{1/2}\right) = 0, \tag{III.12}$$

we find the variational parameter

$$\omega_{\perp} = \frac{\omega_{\perp}^0}{\left(1 + \frac{2Nam^{1/2}}{(2\pi\hbar)^{1/2}}\omega_z^{1/2}\right)^{1/2}} = \frac{\omega_{\perp}^0}{\Delta}, \tag{III.13}$$

where

$$\Delta = \left(1 + \frac{\varsigma^5}{(32\pi^3)^{3/2}}\left(\frac{\omega_z}{\omega_{\perp}^0}\right)^{1/2}\right)^{1/2}. \tag{III.14}$$

Interactions spread out the distribution in the transverse direction by a factor $\Delta^{1/2}$ by reducing the effective transverse oscillator frequency by Δ.

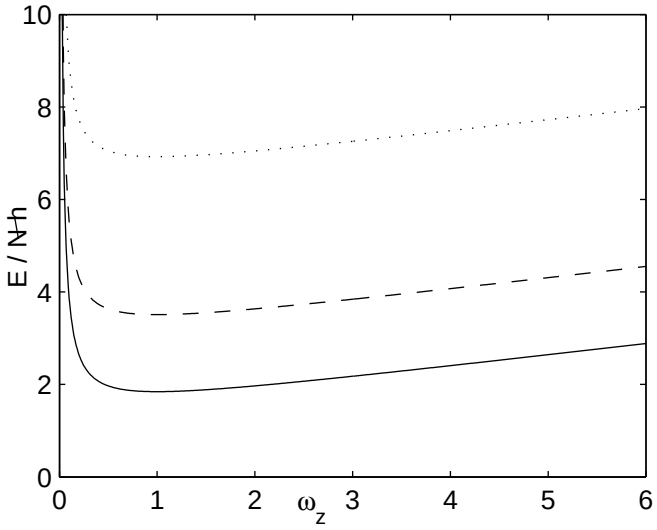

Figure III.2: Energy per particle as a function of ω_z. Curves are plotted for different values of the parameter $N|a|/a_\perp$. Solid line stands for the largest value of the interaction strength.

Spreading in the z-direction begins to become significant when the interaction energy per particle becomes comparable with $\hbar\omega_z^0$. Substituting equation (III.13) into equation (III.11) we get

$$E[\omega_z] = N\hbar\left(\omega_\perp^0\Delta + \frac{\omega_z}{4} + \frac{(\omega_z^0)^2}{4\omega_z}\right). \tag{III.15}$$

We employ the Binomial expansion to the Δ and neglect the second and higher order terms. Equating the first derivative of $E(\omega_z)$ to zero one finds $\omega_z^2 = (\omega_z^0)^2$. Using this result in the second derivative of $E(\omega_z)$ we get the condition $Na/a_\perp \geq (\omega_z^0/\omega_\perp^0)^{1/2}$. From Figure III.2, one can see that as the interaction strength increases the minimum of the energy lowered.

III.2.1 Thomas-Fermi Approximation

The limit of large N is particularly interesting since this condition is well satisfied in most of the current experiments. Moreover, in this limit mean-field theory

takes a rather simple analytic form.

As N increases, the atoms are pushed outwards, the central density becomes flat and the radius grows. As a result, the kinetic energy term in the stationary GP equation (II.32) takes a significant contribution only near the boundary and becomes less important than the interaction energy. Neglecting the kinetic energy in equation (II.32) completely, we get the density profile in the form

$$\rho(\mathbf{r}) = \varphi^2(\mathbf{r}) = g^{-1}[\mu - V_{ext}(\mathbf{r})] \tag{III.16}$$

in the region where $\mu > V_{ext}(\mathbf{r})$ and $\rho = 0$ outside. This is referred to Thomas-Fermi (TF) approximation. This form is acceptable except where the density is small, in which case the contribution of the kinetic energy is important.

If we impose the normalization condition on $\rho(\mathbf{r})$ and substitute $V_{ext}(\mathbf{r}) = m[(\omega_\perp^0)^2 r_\perp^2 + (\omega_z^0)^2 z^2]/2$ into this we obtain

$$N = \int g^{-1}\left[\mu - \frac{m}{2}[(\omega_\perp^0)^2 r_\perp^2 + (\omega_z^0)^2 z^2]\right]\theta\left[\mu - \frac{m}{2}[(\omega_\perp^0)^2 r_\perp^2 + (\omega_z^0)^2 z^2]\right] d^3r, \tag{III.17}$$

where θ is the unit step function. Employing change of variables $\alpha = \omega_\perp^0 r_\perp$, $\beta = \omega_z^0 z$ and $\alpha^2 + \beta^2 = r^2$ the Equation (III.17) takes the form,

$$N = \frac{2\pi}{g(\omega_\perp^0)^2\omega_z^0}\int_0^\infty \left(\mu - \frac{m}{2}r^2\right)\theta\left[\mu - \frac{m}{2}r^2\right] r^2 dr. \tag{III.18}$$

Taking this integral and making some simplification we get the relation between the chemical potential and the number of particles as

$$\mu = \frac{\hbar\omega_\perp^0}{2}\left(\frac{15\lambda N a}{a_\perp}\right)^{2/5}, \tag{III.19}$$

where $\lambda = \omega_z^0/\omega_\perp^0$.

Since $\mu = dE/dN$,

$$E = \int \frac{\hbar\omega_\perp^0}{2}\left(\frac{15\lambda a}{a_\perp}\right)^{2/5} N^{2/5} dN \tag{III.20}$$

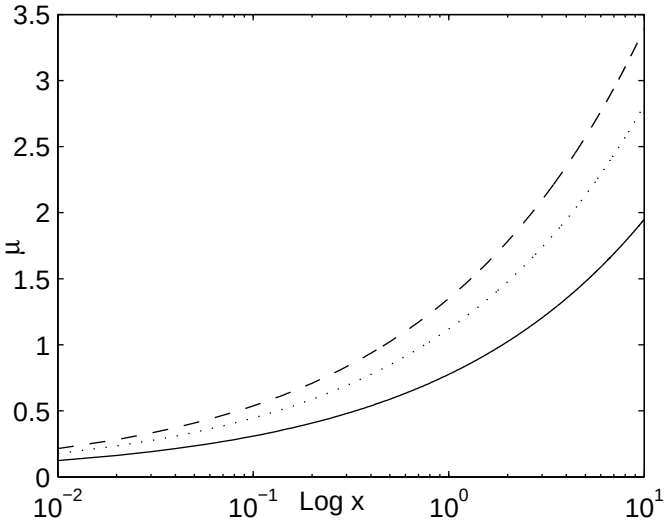

Figure III.3: TF chemical potential,in units of $\hbar\omega_\perp^0$, as a function of interaction strength ($x = Na/a_\perp$).Curves are plotted for several values of λ. Solid line shows the largest value, $\lambda = 1$.

and the energy per particle turns out to be

$$\frac{E}{N} = \frac{5}{7}N\mu. \tag{III.21}$$

This energy is the sum of the interaction and oscillator energies, since the kinetic energy has no contribution for large N. One can see from the Figure III.3 that when the trap is spherically symmetric i.e. $\lambda = 1$ the chemical potential has the minimum value.

The density profile (III.16) has a form of inverted parabola which vanishes at the classical turning point (R, Z). The widths in the radial and axial directions are fixed by the conditions $\mu = m(\omega_\perp^0)^2R^2/2 = m(\omega_z^0)^2Z^2/2$. Then the transverse radius of the cloud is

$$\frac{R}{a_\perp} = \left(\frac{15\lambda Na}{a_\perp}\right)^{2/5} \tag{III.22}$$

and the half height in $Z-$direction is $Z = R/\lambda$. Te value of the density (III.16)

at the center of the trap is $\rho_{TF}(0) = \mu/g$,

$$\rho_{TF}(0) = \frac{1}{8\pi a_\perp^2 a}\left(\frac{15\lambda N a}{a_\perp}\right)^{2/5} = \left(\frac{15\lambda}{8\pi}\right)\frac{N}{a_\perp^3 \varsigma^3}. \tag{III.23}$$

This density is much lower than the one for the noninteracting particles. Using the equation (III.7) we get $\rho_{ho} = N/\pi^{3/2} a_\perp^2 a_z$. The ratio between the central densities is

$$\frac{\rho_{TF}(0)}{\rho_{ho}(0)} = \frac{\pi^{1/2} 15^{2/5} \lambda^{1/2}}{8}\left(\frac{N\lambda a}{a_\perp}\right)^{-3/5} \tag{III.24}$$

and decreases with N. Inclusion of kinetic energy corrections spreads the distribution and decreases the density.

If R is much larger than the healing length, the quantum pressure term becomes negligible. If we substitute the central density into the healing length (II.35) we get

$$\frac{\xi}{R} = \left(\frac{a_\perp}{R}\right)^2 = \left(\frac{15\lambda N a}{a_\perp}\right)^{-2/5}. \tag{III.25}$$

The above equation shows that the healing length decreases with N. Therefore Thomas-Fermi approximation is valid for the large N limit.

CHAPTER IV

LOW DIMENSIONAL BOSE GAS

In this chapter, two and one-dimensional Bose gases are studied. We show that there are no Bose-Einstein condensation in a 2D and 1D uniform Bose gases in Section IV.1. The ideal Bose gases confined in harmonic and power-law potentials are examined. The condensate fractions, critical temperatures and the energies per particle are calculated. Finally we studied the properties of BEC in highly anisotropic trap in effective 2D and 1D. The total energy and the chemical potential are calculated by using a variational approach in cigar and pancake geometries. The conditions for lower dimensionality are derived and theoretical and experimental values of the release energies are compared.

IV.1 Ideal Bose gas in Two- And One-Dimensions

In a uniform gas Bose-Einstein condensation cannot occur in one and two-dimensions because thermal fluctuations destabilize the system. In the presence of BEC, the chemical potential equals to zero for an ideal gas and the momentum distribution is

$$n(p) \propto [\exp(\beta p^2/2m) - 1]^{-1}. \tag{IV.1}$$

It can be seen that in the thermodynamic limit this violates the normalization condition, i.e. $\int n(p)dp$ diverges. Then Bose-Einstein condensation is impossible in 2D and 1D in uniform systems. But it should occur in atom traps since the confining potential modifies the density of states.

IV.2 Harmonic Potential

IV.2.1 Two-Dimensional Bose Gas

The confining potential can be written as

$$V_{ext}(\mathbf{r}) = \frac{1}{2}m\omega^2 r^2, \tag{IV.2}$$

where $r^2 = x^2 + y^2$ and $\omega = (\omega_x\omega_y)^{1/2}$.

By neglecting atom-atom interactions we can write the eigenvalues of the many-body Hamiltonian as

$$\epsilon_{n_x n_y} = (n_x + n_y + 1)\hbar\omega. \tag{IV.3}$$

At temperature T, the total number of particles is given in grand-canonical ensemble

$$N = \sum_{n_x,n_y} \frac{1}{\exp[\beta(\epsilon_{n_x n_y} - \mu)] - 1} \tag{IV.4}$$

and the total energy is

$$E = \sum_{n_x,n_y} \frac{\epsilon_{n_x n_y}}{\exp[\beta(\epsilon_{n_x n_y} - \mu)] - 1}. \tag{IV.5}$$

Similar to 3-dimensional case we separate out the lowest eigenvalue ϵ_{00} from the sum and call N_0 as the number of particle in this state. When the chemical potential equals to the ϵ_{00} i.e. $\mu \to \mu_c = \hbar\omega$, this number can be macroscopic.

$$N - N_0 = \sum_{n_x,n_y\neq 0} \frac{1}{\exp[\beta\hbar\omega(n_x + n_y)] - 1}. \tag{IV.6}$$

This summation can be replaced by an integral as $N \to \infty$,

$$N - N_0 = \int_0^\infty \frac{dn_x dn_y}{\exp[\beta\hbar\omega(n_x + n_y)] - 1}. \tag{IV.7}$$

By making change of variables $\tilde{n} = \beta\hbar\omega n_x$ etc. and using the definition of Riemann Zeta function (Appendix A), this integral yields

$$N - N_0 = \left(\frac{k_B T}{\hbar\omega}\right)^2 \zeta(2). \tag{IV.8}$$

At the transition $N_0 \to 0$ then the critical temperature is,

$$k_B T_c^{2D} = \hbar\omega \left(\frac{N}{\zeta(2)}\right)^{1/2}. \tag{IV.9}$$

For $T < T_c$, the condensate fraction can be calculated by substituting the critical temperature into equation(IV.8)

$$\frac{N_0}{N} = 1 - \left(\frac{T}{T_c^{2D}}\right)^2. \tag{IV.10}$$

It can be obtained also by using the density of states $\rho(\epsilon) = \epsilon/(\hbar\omega)^2$. The total energy is also calculated with this density of states as,

$$E = \int_0^\infty \frac{\rho(\epsilon)\epsilon d\epsilon}{\mathrm{e}^{\beta\epsilon} - 1}. \tag{IV.11}$$

By changing of variables and substituting the critical temperature we find the total energy as

$$\frac{E}{N k_B T_c^{2D}} = \frac{2\zeta(3)}{\zeta(2)} \left(\frac{T}{T_c^{2D}}\right)^3. \tag{IV.12}$$

From this energy the specific heat is obtained as,

$$C_V = N k_B \frac{6\zeta(3)}{\zeta(2)} \left(\frac{T}{T_c^{2D}}\right)^2. \tag{IV.13}$$

In the Figure IV.1 the condensate fractions of ideal Bose gas confined in harmonic trap in $3D$ and $2D$ is shown.

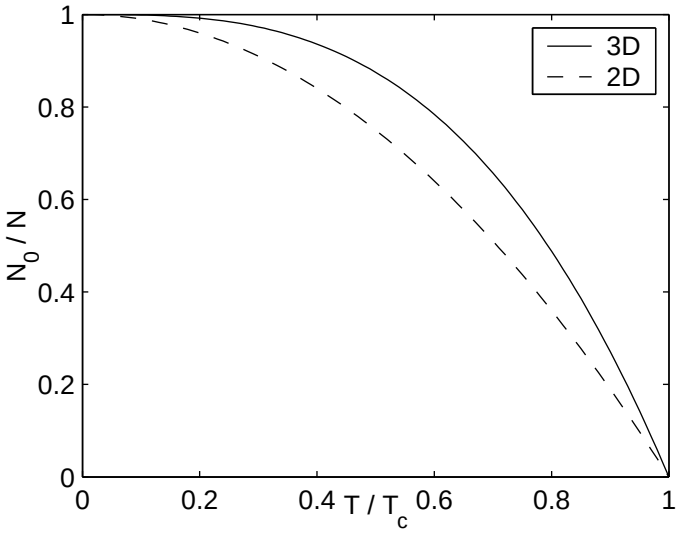

Figure IV.1: Condensate fractions as a function of T/T_c for 3- and 2-dimensional ideal Bose gas trapped in harmonic potential.

IV.2.2 One-Dimensional Bose Gas

In Section IV.1 we said that Bose-Einstein condensation can occur in atom traps but in one-dimension BEC cannot occur in a harmonic trap. One can see this by calculating the condensate fraction. Similar to the two-dimensional case one can find that

$$N - N_0 = \frac{k_B T}{\hbar\omega}\zeta(1). \tag{IV.14}$$

Recalling the properties of the Riemann Zeta function (A), $\zeta(s)$ diverges for $s \leq 1$. The Equation (IV.14) diverges. This means that in the thermodynamic limit the critical temperature for one-dimensional Bose gas tends to zero.Despite the fact that there is no BEC in thermodynamic limit there can be observed two-step BEC for finite values of N.

IV.3 Power-Law Potential

IV.3.1 Two-Dimensional Bose Gas

In this part, we examine the 2D Bose gas confined in power-law potentials because these potentials lead to analytical solutions and most of the traps display power-law behavior close to their minimum. The most general potential is given in the form [37]

$$V_{ext}(x,y) = V_1 \left(\frac{x}{b}\right)^m + V_2 \left(\frac{y}{c}\right)^n . \tag{IV.15}$$

For simplicity we assume that the potential is isotropic,

$$V_{ext}(r) = V_0 \left(\frac{r}{a}\right)^\eta . \tag{IV.16}$$

By using the definition

$$\rho(\epsilon) = \left(\frac{m}{2\pi\hbar^2}\right) \frac{1}{\Gamma(1)} \int [\epsilon - V_{ext}(r)] dr, \tag{IV.17}$$

for the density of states we get

$$\rho(\epsilon) = \frac{2\pi m}{h^2} \int_0^{r*} 2\pi r dr, \tag{IV.18}$$

where $r* = a(\epsilon/V_0)^{1/\eta}$. The density of states is obtained as,

$$\rho(\epsilon) = \frac{2\pi^2 m a^2}{h^2} \left(\frac{\epsilon}{V_0}\right)^{2/\eta} . \tag{IV.19}$$

By using this result one can calculate the total number of particles as

$$N = N_0 + \frac{2\pi^2 m a^2}{h^2 V_0^{2/\eta}} \int_0^\infty \frac{\epsilon^{2/\eta} d\epsilon}{\mathrm{e}^{(\epsilon-\mu)/\mathrm{k_B T}} - 1}. \tag{IV.20}$$

Using $y = \epsilon/k_B T$, we obtain,

$$N = N_0 + \frac{2\pi^2 m a^2}{h^2 V_0^{2/\eta}} (k_B T)^{\frac{2}{\eta}+1} g_2(\eta, \mu/k_B T), \tag{IV.21}$$

where the 2D Bose function is

$$g_2(\eta, x) = \int_0^\infty \frac{y^{2/\eta} dy}{\mathrm{e}^{\mathrm{y-x}} - 1}. \tag{IV.22}$$

For $\mu = 0$ i.e. at T_c,

$$g_2(\eta, 0) = \Gamma\left(\frac{2+\eta}{\eta}\right) \zeta\left(\frac{2+\eta}{\eta}\right). \tag{IV.23}$$

$g_2(\eta, 0)$ remains finite for all positive values of η. So that Bose-Einstein condensation can always occur in an ideal two-dimensional gas confined by a power-law trap. The limit $\eta \to \infty$ corresponds to a rigid box. $g_2(\infty, 0)$ diverges and BEC does not occur.

At transition $N_0 = 0$, then the critical temperature is

$$k_B T_c^{2D} = \left[\frac{N h^2 V_0^{2/\eta}}{2\pi^2 m a^2 g_2(\eta, 0)}\right]^{\eta/2+\eta}. \tag{IV.24}$$

The total energy is found as

$$\frac{E}{N k_B T_c^{2D}} = \frac{\Gamma\left(\frac{2+2\eta}{\eta}\right) \zeta\left(\frac{2+2\eta}{\eta}\right)}{\Gamma\left(\frac{2+\eta}{\eta}\right) \zeta\left(\frac{2+\eta}{\eta}\right)} \left(\frac{T}{T_c^{2D}}\right)^{\frac{2+2\eta}{\eta}}, \tag{IV.25}$$

and the specific heat is given by

$$C_V = N k_B \left(\frac{2+2\eta}{\eta}\right) \frac{\Gamma\left(\frac{2+2\eta}{\eta}\right) \zeta\left(\frac{2+2\eta}{\eta}\right)}{\Gamma\left(\frac{2+\eta}{\eta}\right) \zeta\left(\frac{2+\eta}{\eta}\right)} \left(\frac{T}{T_c^{2D}}\right)^{\frac{2+\eta}{\eta}}. \tag{IV.26}$$

One can see that when $\eta = 2$ i.e. harmonic trap, results are the same with that of the previous calculations for the harmonic trap.

IV.3.2 One-Dimensional Bose Gas

We consider an one-dimensional gas confined by a power-law potential

$$V_{ext}(x) = V_0 \left(\frac{|x|}{L}\right)^\eta. \tag{IV.27}$$

The density of states can be calculated from the definition [37]

$$\rho(\epsilon) = \frac{\sqrt{2m}}{h} \int_{-l(\epsilon)}^{l(\epsilon)} \frac{dx}{\sqrt{\epsilon - V_{ext}(x)}}, \tag{IV.28}$$

where $2l(\epsilon)$ is the available length for particles with energy ϵ, $l(\epsilon) = L(\epsilon/V_0)^{1/\eta}$. Using $y = V_0|x|^\eta/\epsilon L^\eta$, we get

$$\rho(\epsilon) = \frac{2\sqrt{2m}}{\eta h} \frac{\epsilon^{1/\eta - 1/2}}{V_0^{1/\eta}} F(\eta), \tag{IV.29}$$

where

$$F(\eta) = \int \frac{y^{(1-\eta)/\eta}\, dy}{\sqrt{1-y}}. \tag{IV.30}$$

By using the result for density of states the total number of particles can be written as

$$N = N_0 + \frac{2L\sqrt{2m}}{\eta h} \frac{F(\eta)}{V_0^{1/\eta}} \int_0^\infty \frac{\epsilon^{1/\eta - 1/2}}{\mathrm{e}^{(\epsilon-\mu)/\mathrm{k_B T}} - 1}\, d\epsilon. \tag{IV.31}$$

We get the result

$$N = N_0 + \frac{2L\sqrt{2m}}{\eta h} \frac{F(\eta)}{V_0^{1/\eta}} (k_B T)^{1/\eta + 1/2} g_1(\eta, \mu/k_B T), \tag{IV.32}$$

where

$$g_1(\eta, x) = \int_0^\infty \frac{y^{1/\eta - 1/2\, dy}}{\mathrm{e^{y-x}} - 1}, \tag{IV.33}$$

is the one-dimensional Bose function.

As T increases $N_0 \sim 0$. As T decreases the chemical potential increases and reaches 0 at some T_c. For $T < T_c$, μ remains zero and N_0 increase.

The function $g_1(\eta, 0)$ can be written in Gamma and Riemann zeta functions

$$g_1(\eta, 0) = \Gamma\left(\frac{1}{\eta} + \frac{1}{2}\right) \zeta\left(\frac{1}{\eta} + \frac{1}{2}\right). \tag{IV.34}$$

One can see that $g_1(\eta, 0)$ remains finite only if $\eta < 2$ from the properties of Riemann zeta function. The 1D ideal Bose gas will display BEC only if the

potential power is less than 2, i.e. only if the external potential is more confining than a parabolic potential.

By setting the number of particles in the ground state zero the critical temperature is obtained as

$$k_B T_c^{1D} = \left[\frac{N\eta h}{2L\sqrt{2m}} \frac{V_0^{1/\eta}}{F(\eta)} \frac{1}{\Gamma\left(\frac{1}{\eta}+\frac{1}{2}\right)\zeta\left(\frac{1}{\eta}+\frac{1}{2}\right)} \right]^{2\eta/(2+\eta)} . \qquad \text{(IV.35)}$$

The value of the factor $(\eta/2)^{2\eta/(2+\eta)}$ is always less than 1 when $0 < \eta < 2$. Therefore, the critical temperature will be suppressed by such a factor.

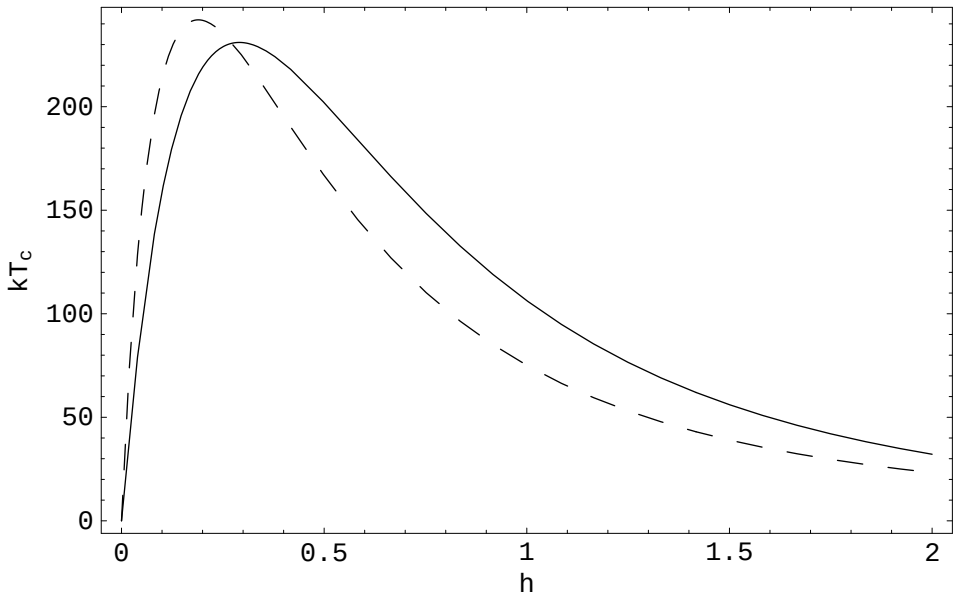

Figure IV.2: Evolution of the critical temperature with the potential parameter η for one- and two-dimensional traps. Solid line stands for $2D$ and dashed line for $1D$.

The total energy is then found as

$$\frac{E}{N k_B T_c^{1D}} = \frac{\Gamma\left(\frac{1}{\eta}+\frac{3}{2}\right)\zeta\left(\frac{1}{\eta}+\frac{3}{2}\right)}{\Gamma\left(\frac{1}{\eta}+\frac{1}{2}\right)\zeta\left(\frac{1}{\eta}+\frac{1}{2}\right)} \left(\frac{T}{T_c^{1D}}\right)^{1/\eta+3/2} , \qquad \text{(IV.36)}$$

and the specific heat

$$C_V = Nk_B \left(\frac{1}{\eta} + \frac{3}{2}\right) \frac{\Gamma\left(\frac{1}{\eta}+\frac{3}{2}\right)\zeta\left(\frac{1}{\eta}+\frac{3}{2}\right)}{\Gamma\left(\frac{1}{\eta}+\frac{1}{2}\right)\zeta\left(\frac{1}{\eta}+\frac{1}{2}\right)} \left(\frac{T}{T_c^{1D}}\right)^{1/\eta+1/2}. \tag{IV.37}$$

In the Figure IV.2 evolution of the critical temperature with the potential power η for 1D and 2D traps is shown. It can be seen that T_c shows a peak between $\eta = 0$ and 2.

IV.4 Effective Lower Dimensions

After the experimental realization of crossover into two-dimensional and one-dimensional condensates [25] there has been a growing interest in Bose-Einstein condensation in effective lower dimensions. Effective lower dimensionality means that excitations along the tightly confined dimension(s) are energetically not allowed for confined gases. This is done by a change in aspect ratio and by the release energy converging to a nonzero value when the number of trapped atoms was reduced.

For condensates in $3D$ an effective and simple analytic description was achieved through the Thomas-Fermi approximation. It is justified for the large number of atoms with aspect ratios of the order of 1. As the aspect ratio is far from unity, the kinetic energy in the constricted direction becomes more important and TF approximation is not valid.

Kunal Das [38] developed a theoretical model which successfully describes condensates from the $3D$ regime with increasing degree of anisotropy all the way to regimes of effective lower dimensionality.

At zero temperature in cylindrical coordinates we can write the energy functional (II.30) as

$$E[\varphi] = N \hbar\omega \int r dr \int dz \left[\frac{\lambda^{1/3}}{2}(|\nabla_r \varphi|^2 + r^2|\varphi|^2) + \frac{\lambda^{-2/3}}{2}(|\nabla_z \varphi|^2 + z^2|\varphi|^2) + \frac{Na}{a_{ho}}|\varphi|^4 \right], \quad \text{(IV.38)}$$

where the aspect ratio is $\lambda = \omega_r/\omega_z$ and $\omega = (\omega_r^2\omega_z)^{1/3}$.

TF approximation gives a value for the chemical potential (III.19) for the condensate with all its spatial dimensions of comparable magnitudes. i.e. $\lambda = 1$,

$$\mu_{TF} = \frac{\hbar\omega}{2}\left(\frac{15Na}{a_{ho}}\right)^{2/5}. \quad \text{(IV.39)}$$

This expression does not depend on the aspect ratio, whereas we would expect that the chemical potential should change as the aspect ratio changes. We use a variational approach again to get the expression for μ that has the correct dependence on the aspect ratio.

IV.4.1 Cigar Geometry

We take the trial wave function [38]

$$\varphi_{cigar}(r,z) = \left(\frac{3\beta_r}{2d^3}\right)^{1/2} \mathrm{e}^{-\beta_\mathrm{r} \mathrm{r}^2/2}\sqrt{\mathrm{d}^2 - \mathrm{z}^2}\,\theta(\mathrm{d}^2 - \mathrm{z}^2), \quad \text{(IV.40)}$$

for the cigar geometry $\lambda \gg 1$, where β_r and d are variational parameters and $\theta(x)$ is the unit step function.

In the axial direction the condensate size far exceeds the oscillator length and the kinetic energy is negligible. We take only the kinetic energy in the transverse direction and neglect that of in the axial direction in the energy functional(IV.38). We obtain,

$$\frac{E}{N\hbar\omega} = \int_0^\infty r\, dr \int_\infty^\infty dz \left[\frac{3\lambda^{1/3}}{4d^3}(\beta_r^2 + \beta_r) r^2 \mathrm{e}^{-\beta_\mathrm{r}\mathrm{r}^2}(\mathrm{d}^2 - \mathrm{z}^2)\theta(\mathrm{d}^2 - \mathrm{z}^2) + \frac{3\lambda^{-2/3}\beta_r^2}{2d^3} z^2 \mathrm{e}^{-\beta_\mathrm{r}\mathrm{r}^2}(\mathrm{d}^2 - \mathrm{z}^2)\theta(\mathrm{d}^2 - \mathrm{z}^2) + \frac{9\beta_\mathrm{r}^2 \mathrm{Na}}{4\mathrm{d}^6 \mathrm{a}_\mathrm{ho}} \mathrm{e}^{-2\beta_\mathrm{r}\mathrm{r}^2}(\mathrm{d}^2 - \mathrm{z}^2)^2\theta(\mathrm{d}^2 - \mathrm{z}^2) \right]. \quad \text{(IV.41)}$$

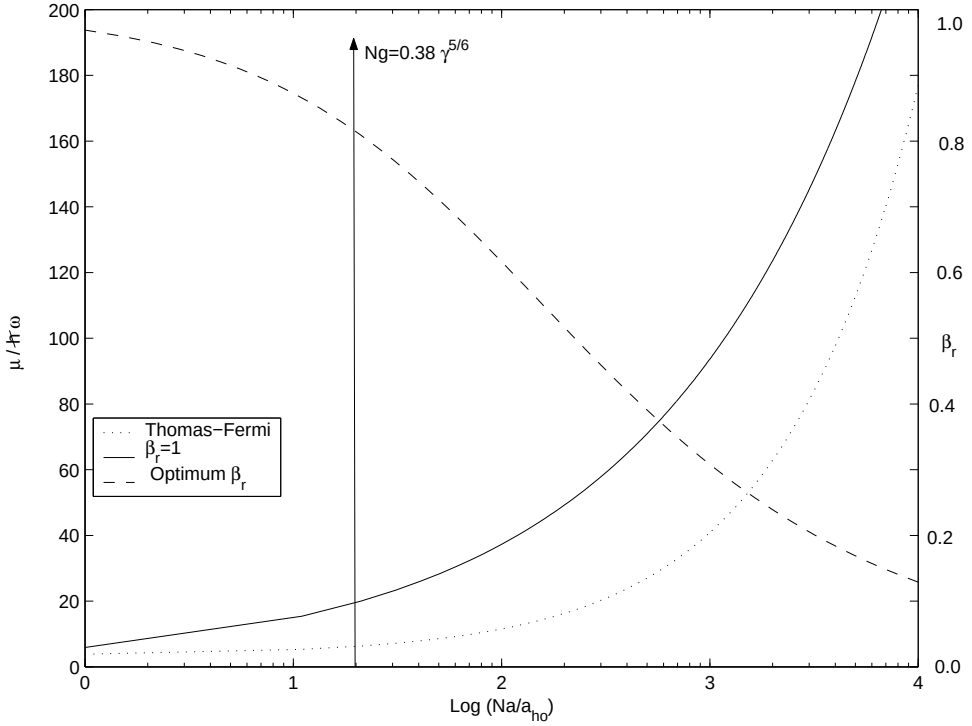

Figure IV.3: Comparison of chemical potential obtained from different approaches as a function of the dimensionless parameter Na/a_{ho} with $\lambda = 100$.

This integral can be written as the sum of three integrals.$I = I_1 + I_2 + I_3$. After calculations we get

$$\frac{E[d,\beta_r]}{N\hbar\omega} = \frac{\lambda^{1/3}}{2}\left(\beta_r + \frac{1}{\beta_r}\right) + \frac{\lambda^{-2/3}}{10}d^2 + \frac{3\beta_r Na}{5da_{ho}}. \tag{IV.42}$$

We minimize E with respect to β_r and d, finally we get the relations

$$\frac{1}{\beta_r^2} = 1 + \frac{6Na}{5da_{ho}}\lambda^{-1/3}, \tag{IV.43}$$

and

$$d^3 = \frac{3\beta_r Na}{a_{ho}}\lambda^{2/3}. \tag{IV.44}$$

We can find the chemical potential corresponding the optimum parameters

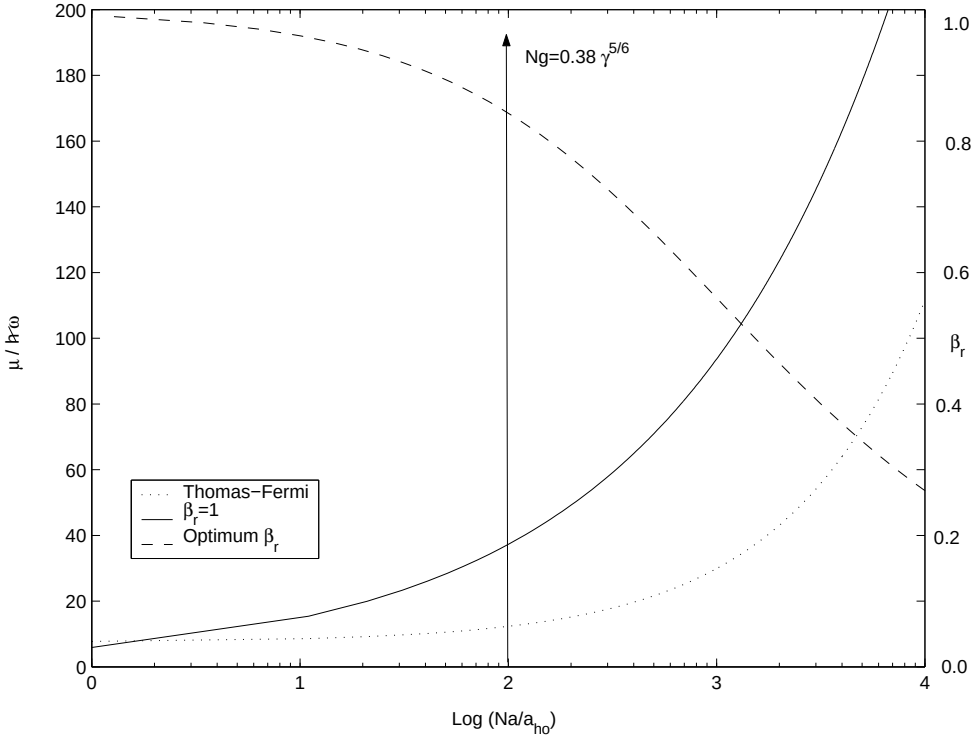

Figure IV.4: Comparison of chemical potential obtained from different approaches as a function of the dimensionless parameter Na/a_{ho} with $\lambda = 1000$.

by taking the derivative of energy with respect to N and we obtain

$$\begin{aligned} \mu &= \hbar\omega \left[\frac{\lambda^{1/3}}{2} \left(\beta_r + \frac{1}{\beta_r} \right) + \frac{1}{2} \left(\frac{3\beta_r Na}{\lambda^{1/3} a_{ho}} \right)^{2/3} \right] \\ &= \frac{\hbar\omega_r}{2} \left(\beta_r + \frac{1}{\beta_r} \right) + \frac{1}{2} (3\beta_r Na\omega_r\omega_z\hbar\sqrt{m})^{2/3}. \end{aligned} \tag{IV.45}$$

It is clearly seen that the last term ($\propto \omega_z^{2/3}$) vanishes in the limit $\omega_z \to 0$, also in that limit $\beta_r \to 1$ so that the chemical potential equals the transverse ground state energy $\hbar\omega_r$.

In order to test the accuracy and validity of this approximation we compare the analytic expressions for the chemical potential with accurate numerical solution of the GP equation obtained by K. Das [38]. He used discrete variable

representation (DVR) mesh in r (Laguerre DVR) and z (Hermite DVR). It is seen that the variational chemical potential with optimized β_r closely follows the numerically computed chemical potential over a large range of Na/a_{ho}. For low densities, the expression with $\beta_r = 1$ is sufficient but it fails as the density increases. However TF expression (IV.39) is accurate at high densities and breaks down at low densities since it approaches zero while the correct chemical potential approach the zero-point energy.

IV.4.2 Disk Geometry

For the disk geometry $\lambda \ll 1$ and we take the trial wave function [38]

$$\varphi_{pan}(r,z) = \frac{2}{b^2}\left(\frac{\beta_z}{\pi}\right)^{1/4} \mathrm{e}^{-\beta_z \mathrm{z}^2/2}\sqrt{\mathrm{b}^2-\mathrm{r}^2}\,\theta(\mathrm{b}^2-\mathrm{r}^2). \tag{IV.46}$$

Similar to the cigar geometry, neglecting the transverse kinetic energy we find,

$$\frac{E}{N\hbar\omega} = \frac{\lambda^{1/3}b^2}{6} + \frac{\lambda^{-2/3}}{4}\left(\beta_z + \frac{1}{\beta_z}\right) + \frac{8Na}{3b^2 a_{ho}}\sqrt{\frac{\beta_z}{2\pi}}. \tag{IV.47}$$

We then get the relations for the optimum parameters that minimize the energy

$$b^4 = \frac{16Na}{\lambda^{1/3}a_{ho}}\sqrt{\frac{\beta_z}{2\pi}}, \tag{IV.48}$$

and

$$\frac{1}{\beta_z^2} = 1 + \frac{16Na\lambda^{2/3}}{3\sqrt{2\pi\beta_z}b^2 a_{ho}}. \tag{IV.49}$$

The corresponding expression for the chemical potential is

$$\mu = \hbar\omega\left[\frac{\lambda^{-2/3}}{4}\left(\beta_z + \frac{1}{\beta_z}\right) + \sqrt{\frac{\lambda^{1/3}Na}{a_{ho}}}\left(\frac{8\beta_z}{\pi}\right)^{1/4}\right]. \tag{IV.50}$$

If we compare the analytic expression for the chemical potential with numerical result of K. Das [38], it is clear that variational expression from Equation

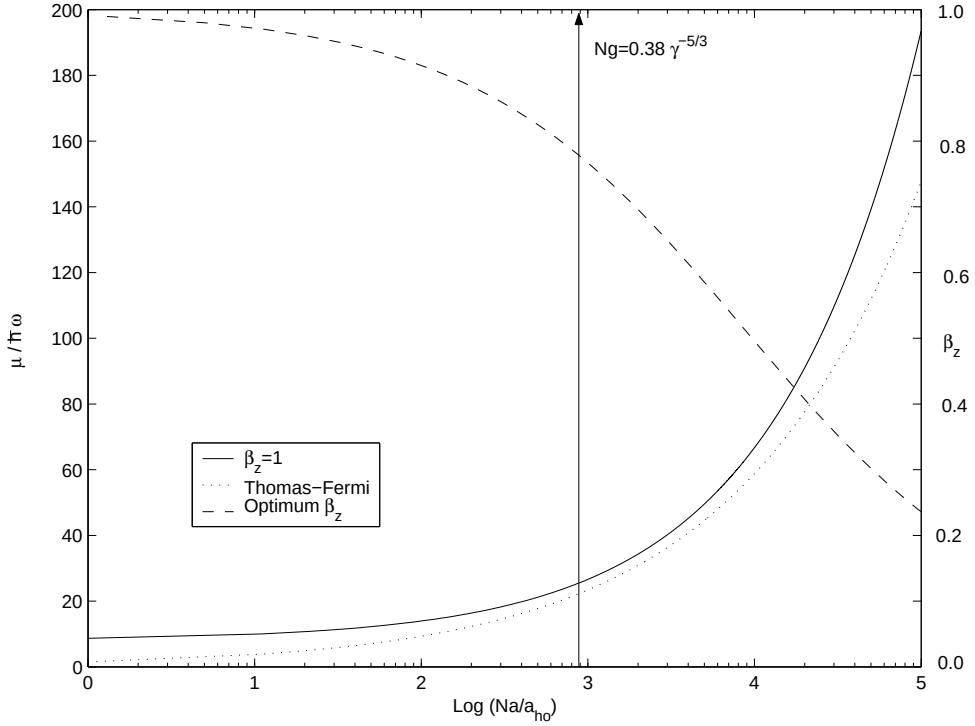

Figure IV.5: The chemical potential for disk shaped traps as a function of the dimensionless interaction strength Na/a_{ho}, obtained from various approaches,for aspect ratio $\lambda = 0.01$.

(IV.50) reproduces almost exactly the numerical solution of the GP equation over the range of Na/a_{ho} shown. The reason for the better agreement is the larger relative importance of the kinetic energy in the tightly confined direction. It is more clearly seen that TF expression (IV.39) fails as the density decreases.

IV.4.3 Crossover To Lower Dimensions

The variational parameters used to obtain the chemical potential also give a measure of the effective dimensionality of the condensate. As discussed in Section IV.4 if excitations in the tightly confined dimension are frozen a trapped

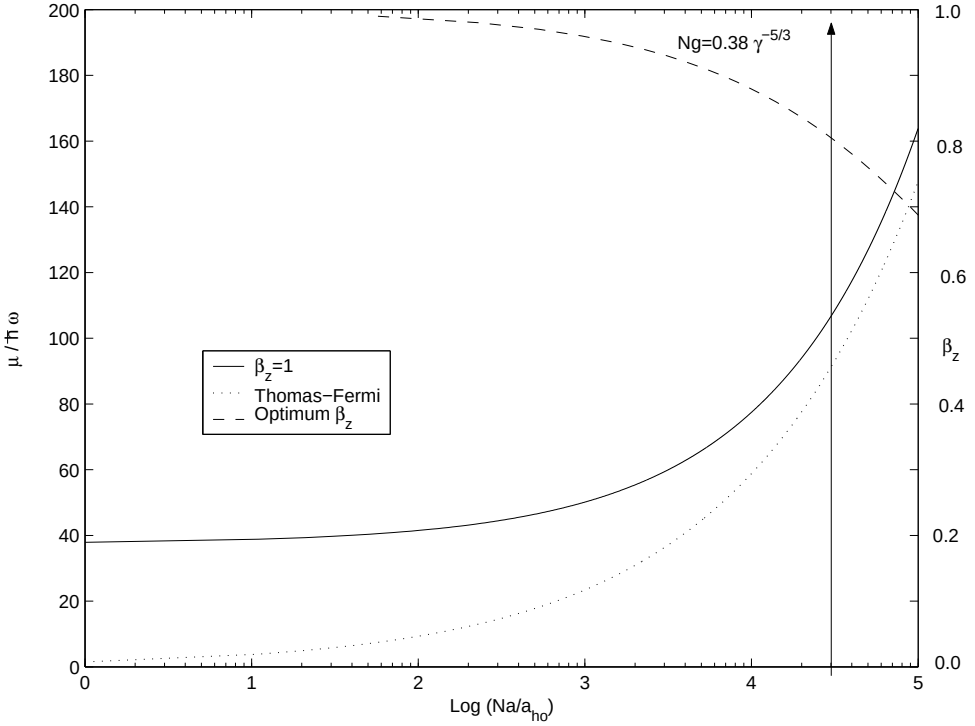

Figure IV.6: The chemical potential for disk shaped traps as a function of the dimensionless interaction strength Na/a_{ho}, obtained from various approaches,for aspect ratio $\lambda = 0.001$.

Bose gas is considered to be in effective lower dimension. For a weakly interacting gas at low densities, the interaction energy can be assumed to be equal to Thomas-Fermi chemical potential. The crossover to 1D and 2D is defined by $\mu_T F \sim \hbar\omega_t$, i.e. when the interaction energy per particle is comparable to the energy to excite in the tightly confined direction. Then the condition for lower dimensionality is

$$\begin{aligned} \frac{N_{1D}a}{a_{ho}} &\sim 0.38\lambda^{5/6}, \\ \frac{N_{2D}a}{a_{ho}} &\sim 0.38\lambda^{-5/3}. \end{aligned} \tag{IV.51}$$

In Figures IV.3, IV.4, IV.5, IV.6 the optimum values of β_r and β_z is plotted

along the right axis. The values corresponding to the crossover to one dimension and to the two dimensions are indicated. One can see that this corresponds to $\beta_r \sim 0.8$ and $\beta_z \sim 0.8$. Thus, the values of β_r and β_z give a measure of the dimensionality of the system. When $\beta_r \sim 1$ the system is effectively one-dimensional since the transverse profile of the condensate coincides with that of the transverse ground state and when $\beta_z \sim 1$ the system is effectively two-dimensional. The system approaches three dimensionality when these parameters deviate from unity.

In the experiment in [25], the crossover from a $3D$ to lower dimensionality was deduced by observing a sudden change in the aspect ratio of the released condensate when the number of atoms was lowered below a certain value, and by observing a saturation of the release energy at the zero-point kinetic energy in the tightly confined direction. One can estimate the release energy in this variational model and compare it with the experimentally observed value due to the conservation of energy.

The release energy is the energy of the system after the traps are switched off. It is just the sum of the kinetic and the interaction energies of the condensate before release. For the cigar geometry $\lambda \gg 1$, the release energy per particle is found by using the Equation (IV.42),

$$E_{rel} = \frac{\hbar\omega_r\beta_r}{2} + \frac{\hbar\omega_z d^2}{5}, \tag{IV.52}$$

where we use the optimized parameters β_r and d in Section IV.4.1.

The release energy in [25] is plotted as a function of the half length (Z) of the condensate. The axial expansion in the $1D$ experiment was negligible within the time of flight till measurement so that we need for comparison the initial half length before release.

The parameter d can be assumed to be half length of the condensate by investigating the form of trial function (IV.40). The half length in $1D$ limit is

obtained by $d(\beta_r = 1 \rightarrow Z_{1D})$. In $3D$ limit, we note that $1/\sqrt{\beta_r}$ is the width of the transverse variational profile and in the expression (IV.43) for β_r measures the deviation from one-dimension. As the condensate moves away from the $1D$ regime and approaches an ellipsoid shape, that deviation would be maximum at the center and negligible at the end of the ellipsoid. Thus we take an average value for the deviation and define the modified $\overline{\beta_r}$ as

$$\frac{1}{\overline{\beta_r}^2} = 1 + \frac{3Na\lambda^{-1/3}}{5a_{ho}d}. \tag{IV.53}$$

In the $3D$ limit $\overline{\beta_r} \ll 1$, we can write $\overline{\beta_r}^2 \simeq \frac{5a_{ho}d\lambda^{1/3}}{Na}$. Then we get the correct limit $d(\overline{\beta_r}) \rightarrow Z_{3D} = \left(\frac{15Na\lambda^{5/3}}{a_{ho}}\right)^{1/5}$.Similarly for $1D$ $d(\overline{\beta_r} = 1) \rightarrow Z_{1D} = \left(\frac{3Na\lambda^{2/3}}{a_{ho}}\right)^{1/3}$. Thus in the intermediate regime we expect the half length to be given a good approximation by

$$Z = \frac{3Na}{a_{ho}}\overline{\beta_r}\lambda^{2/3}. \tag{IV.54}$$

The release energy should be evaluated with the optimized variational parameters. The variational process optimizes energy and not condensate dimensions hence there is no inconsistency.

In Figure IV.7 the release energy per particle is plotted as a function of the half length from Equation (IV.54). The parameters are the same with those in the experiment [25]; sodium atoms in a magnetic trap with $\omega_r = 2\pi \times 360Hz$ and $\omega_z = 2\pi \times 3.5Hz$ so that the aspect ratio is $\lambda \simeq 103$. Comparison with the experimental result shows that the expression (IV.52) for the release energy close to their measured data; as the system approaches effective $1D$ the saturation of the release energy at the radial zero-point energy is clear.

In the disk geometry the release energy per particle is founded similarly

$$E_{rel} = \frac{\hbar\omega_z\beta_z}{4} + \frac{\hbar\omega_r b^2}{6}. \tag{IV.55}$$

We cannot compare the above expression with the experimental data. Since the trap in $2D$ experiment had not strictly cylindrical geometry and unlike $1D$ case

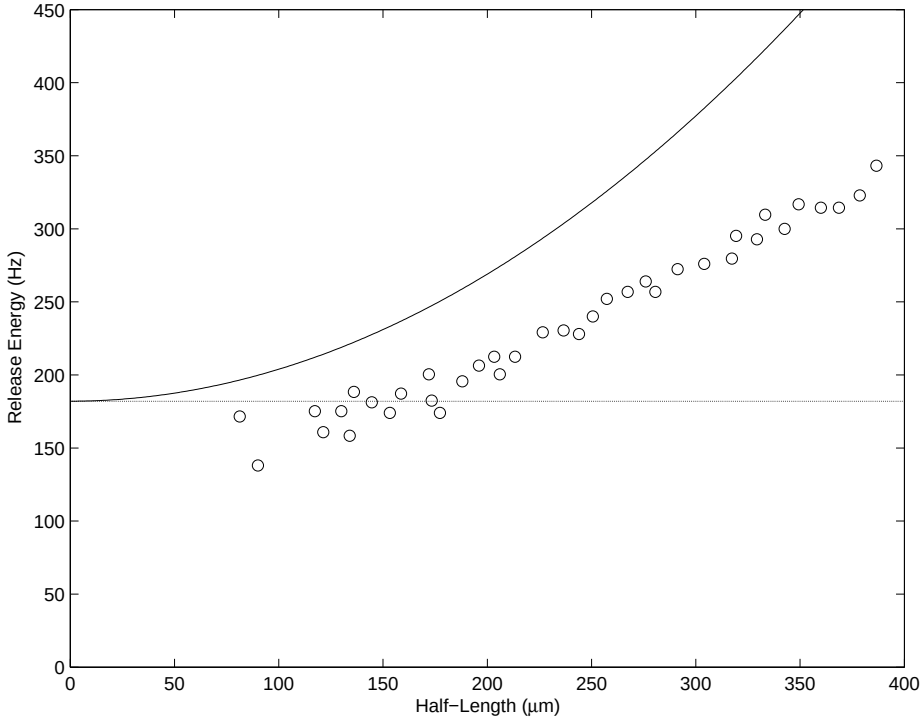

Figure IV.7: The release energy per particle $E_{rel}/\hbar$ as a function of the half length of a cigar shaped condensate. The horizonal line represents the transverse zero-point energy.The experimental data obtained by Görlitz[25] is shown by bubles.

there is significant expansion of the condensate in all directions till the time of measurement which involves the dynamics of expansion.

CHAPTER V

CONCLUSION

The study of the three-dimensional Bose gas confined by harmonic potential is very important. Because the shape of the trapping potential is well approximated by a harmonic shape in many experiments. In studying weakly interacting systems, the Gross-Pitaevskii equation, which is non-linear, is used. Since it is non-linear, one can not solve it analytically but numerical and variational approaches are available. We employed the variational approach which gives an upper bound for the ground state energy. Comparing the numerical and the variational results, it is seen that they are consistent for the systems under consideration. We showed how a nonuniform confinement and two-body interactions characterize the ground state properties of the system. It is shown that if the interatomic forces are attractive ($a < 0$) the central density increases. If it grows too much, the gas will collapse. We calculated the N_{cr} for the collapse by means of variational approach. It is shown that above N_{cr} the local minimum of the energy disappears and the Gross-Pitaevskii equation has no solution.

The repulsive interaction ($a > 0$) case is also examined. In this case an

effective and simple analytic description was achieved through the Thomas-Fermi approximation. It is shown that Thomas-Fermi approximation is valid for large condensates with aspect ratios of the order of unity.

The study of one- and two-dimensional systems is very important because in lower dimensions Bose-Einstein condensation shows new features which modify the behavior of the system. It is shown that BEC is impossible in $1D$ and $2D$ in a homogeneous system but occurs in atom traps. The critical temperatures and the condensate fractions are calculated for the $1D$ and $2D$ nonuniform gases. It is also shown that the one-dimensional Bose gas display BEC only if the external potential is more confining than a parabolic potential.

A simple model is given to describe how a condensate changes as it becomes more anisotropic and crosses over to effective lower dimensionality. Comparison with the numerical solutions shows that this model is accurate and valid. By using a variational approach we obtained analytic expressions for the chemical potential which are valid for cylindrical condensates for all degrees of anisotropy even where the Thomas-Fermi approximation is completely inadequate. It is also shown that the variational parameters used to obtain the chemical potential give a measure of the effective dimensionality of the condensate. The expressions for the total energy and the release energy have been found and they are valid in $3D$ as well as in effective one- and two-dimensions. The release energy is shown to agree well with experimentally measured values.

As it is mentioned in Section II.3 the variational method gives an upper bound for the ground state energy. One should employ numerical methods to obtain more accurate results for such nonlinear partial differential equations. Besides the advantage of getting analytic expressions by variational approach, it was also shown in relevant sections that results obtained numerically are closer to those obtained experimentally. Future work should be focus on proper numerical analysis of the problem.

Lower dimensional condensates offer many opportunities for further studies. The one-dimensional case is particularly interesting. Because, the gas becomes an impenetrable Tonks-Girardeau gas at extremely low density and tight confinement. A gas of such impenetrable bosons behaves like a free Fermi gas. However, our variational functions cannot be applied to the Tonks-Girardeau regime, since the Thomas-Fermi profile in the axial direction has to be replaced by a square root of a parabola and the axial energy is simply the Fermi energy for N particles in $1D$. The variational ansatz which is used in our calculations should be useful in studying $2D$ lattices of effective one-dimensional condensates.

Recently, a different approach from variational/perturbative and numerical methods appeared for studying effectively $1D$ Bose gases [42]. This method is based on Lieb-Liniger solution for $1D$ delta-dunction Bose gas. Using this model they investigate the five cases: ideal gas case, $1D$ Gross-Pitaevskii case, $1D$ Thomas-Fermi case, Lieb-Liniger case and Girardeau-Tonks case. It is also presented a $1D$ energy functional, analogous to the Gross-Pitaevskii functional, that correctly describes the energy and density in all of the five cases. Researches are currently using this model to investigate various properties of $1D$ Bose systems [43]. The future work would be done on this model.

REFERENCES

[1] Einstein A., Sitzungsberg k. Preuss. Akad. Wiss. Phys. Math. **K1**, (1925) 3.

[2] Bose S., Z. Phys. **26**, (1924) 178.

[3] Anderson M. H., J. R. Ensher, M. R. Matthews, C. E. Wieman, E. A. Cornell, Science **269**, (1995) 198.

[4] Davis K. B., M. O. Mewes, M. R. Andrews, N. J. von Druten, D. F. Durfee, D. M. Kurn, W. Ketterle, Phys. Rev Lett. **75**, (1995) 3969.

[5] Ketterle W., Rev. Mod. Phys. **74**, (2002) 1131.

[6] Allen J. F., A. D. Misener, Nature **141**, (1938) 75.

[7] Kapitza P. L., Nature **141**, (1938) 913.

[8] London F., Nature **141**, (1938) 643.

[9] Penrose O., Philos. Mag. **42**, (1951) 1373.

[10] Penrose O., L. Onsager, Phys. Rev **104**, (1956) 576.

[11] Cornell E. A., C. E. Wieman, Rev. Mod. Phys. **74**, (2002) 875.

[12] Stwalley W. C., L. H. Nosanow, Phys. Rev. Lett. **36**, (1976) 910.

[13] Silvera I. F., J. T. M. Walraven, Phys. Rev. Lett. **44**, (1980) 164.

[14] Hardy W. N., M. Morrow, R. Jochemsen, A. Berlinsky, Physica B and C **110**, (1982) 1964.

[15] Greytak T. J., D. Kleppner, in *New Trends in Atomic Physics*, edited by G. Grynberg, R. Stora (North Holland, Amsterdam, 1984).

[16] Chu S. *et al.*, Phys. Rev. Lett. **55**, (1985) 48.

[17] Raab E. L. *et al.*, Phys. Rev. Lett. *59*, (1987) 2631.

[18] Pitaevskii L., S. Stringari, *Bose-Einstein Condensation*, (Clarendon Press, Oxford, 2003).

[19] Leanhardt A. E. *et al.*, Science **301**. (2003) 1513.

[20] Bradley C. C. *et al.*, Phys. Rev. Lett. **75**, (1995) 1687.

[21] Fried D. G. *et al.*, Phys. Rev. Lett. **81**, (1998) 3811.

[22] Pereira dos Santos I. *et al.*, Phys. Rev. Lett. **86**, (2001) 3459.

[23] Robert A. *et al.*, Science **292**, (2001) 461.

[24] Modugno G. *et al.*, Science **294**, (2001) 1320.

[25] Gorlitz A., *et al.*, Phys. Rev. Lett. **87**, (2001) 130402-1.

[26] Hohenberg P. C., Phys. Rev. **158**, (1967) 383.

[27] Dalfovo F., S. Giorgini, L. P. Pitaevskii, Rev. Mod. Phys. **71**, (1999) 463.

[28] Ensher J. R., D. S. Jin, M. R. Matthews, C. E. Wiemann, E. A. Cornell, Phys. Rev. Lett. **77**, (1996) 4984.

[29] Schneider B. I., D. L. Feder, Phys. Rev. A **59**, (1999) 2232.

[30] Bogoluibov N., J. Phys. (Moscow) **11**, (1947) 23.

[31] Gross E. P., Nuovo Cimento **20**, (1961) 454.

[32] Gros E. P., J. Math. Phys. **4**, (1963) 195.

[33] Pitaevskii L. P., Sov. Phys. JETP **13**, (1961) 451.

[34] Visintin A.,*Models of Phase Transitions*, (Birkhauser, Boston, 1996).

[35] Ruprecht P. A., M. J. Holland, K. Burnett, M. Edwards, Phys. Rev. A **51**, (1995) 4704.

[36] Baym G., C. J. Pethick, Phys. Rev. Lett. **76**, (1996) 6.

[37] Bagnato V., D. Kleppner, Phys. Rev. A **44**, (1991) 7439; Dai W., M. Xie, Phys. Rev. A **67**, (2003) 027601.

[38] Das K., Phys. Rev. A, **66**, (2002) 053612-1.

[39] Greiner W., Neise L., Stcker H., *Thermodynamics and Statistical Mechanics*, (Springer-Verlag, New York, 1994).

[40] Landau L. D., E. M. Lifshitz, *Statistical Physics*, 2nd Edition (Addison-Wesley, Massachusetts, 1969).

[41] Pathria R. K., *Statistical Mechanics*, 2nd Edition (Butterworth-Heinemann, Oxford, 1996).

[42] Lieb E. H., R. Seiringer, Phys. Rev. Lett. **91**, (2003) 150401.

[43] Astrakharchik G. E., S. Giorgini, Phys. Rev. A **68**, (2003) 031602; Olshanii M., V. Dunjko, Phys Rev Lett. **91**, (2003) 090401.

APPENDIX A

Bose Functions

The general form of the Bose functions is [39]

$$g_\nu(z) = \frac{1}{\Gamma(\nu)} \int_0^\infty \frac{x^{\nu-1} dx}{z^{-1}\mathrm{e}^{\mathrm{x}} - 1} \quad 0 \le z \le 1, \quad \nu \in R \tag{A.1}$$

where $\Gamma(\nu)$ is the Gamma function.

For small z, we can expand the integrand, $z\mathrm{e}^{-\mathrm{x}} \le 1$ in our case $\exp[-\beta(\epsilon - \mu)] \le 1$:

$$\begin{aligned} \frac{1}{z^{-1}\mathrm{e}^{\mathrm{x}} - 1} &= z\,\mathrm{e}^{-\mathrm{x}} \frac{1}{1 - z\mathrm{e}^{-\mathrm{x}}}, \\ &= z\,\mathrm{e}^{-\mathrm{x}} \sum_{\mathrm{k}=0}^{\infty} (z\mathrm{e}^{-\mathrm{x}})^{\mathrm{k}}, \\ &= \sum_{k=1}^{\infty} z^k \mathrm{e}^{-\mathrm{kx}}. \end{aligned} \tag{A.2}$$

Using this result in the equation (A.1) we find

$$g_\nu(z) = \frac{1}{\Gamma(\nu)} \sum_{k=1}^{\infty} z^k \int_0^\infty x^{\nu-1} \mathrm{e}^{-\mathrm{kx}} \mathrm{dx}. \tag{A.3}$$

By changing variables, $y = kx$, we get

$$g_\nu(z) = \frac{1}{\Gamma(\nu)} \sum_{k=1}^{\infty} \frac{z^k}{k^\nu} \int_0^\infty y^{\nu-1} \mathrm{e}^{-\mathrm{y}} \mathrm{dy}. \tag{A.4}$$

The last integral is the definition of Gamma function, then we obtain

$$g_\nu(z) = \sum_{k=1}^{\infty} \frac{z^k}{k^\nu}, \quad 0 \leq z \leq 1. \tag{A.5}$$

For $z = 1(\mu = 0)$, there is relationship to Riemann Zeta function

$$g_\nu(1) = \sum_{k=1}^{\infty} \frac{1}{k^\nu} = \zeta(\nu), \quad \nu > 1, \tag{A.6}$$

where $\zeta(\nu)$ can be also written in the integral form [40]

$$\zeta(\nu) = \frac{1}{\Gamma(\nu)} \int_0^\infty \frac{x^{\nu-1} dx}{\mathrm{e^x} - 1}, \quad \nu > 1. \tag{A.7}$$

This series converges only for $\nu > 1$. This does not mean that the functions $g_\nu(z)$ are defined only for $\nu > 1$, but that $g_\nu(z) \to \infty$ for $\nu \leq 1$ and $z \to 1$. $g_\nu(z)$ is finite for $\nu > 1$ for all $0 \leq z \leq 1$.

Some special values of the often used $\zeta-$functions are listed below:

$$\begin{array}{ccc} \zeta(1) \to \infty & \zeta(3/2) = 2.612 & \zeta(2) \approx 1.645 \\ \zeta(5/2) = 1.341 & \zeta(3) = 1.202 & \zeta(7/2) = 1.127 \\ \zeta(4) \approx 1.082 & \zeta(5) = 1.037 & \zeta(6) \approx 1.017 \\ \zeta(7) = 1.008 & \zeta(8) \approx 1.004 & \end{array} \tag{A.8}$$

A simple differentiation of $g_\nu(z)$ gives the recurrance relation [41]

$$z \frac{\partial}{\partial z}[g_\nu(z)] = \frac{\partial}{\partial (lnz)} g_\nu(z) = g_{\nu-1}(z). \tag{A.9}$$

This relation follows from the series expansion (A.6).